Discover Mechanical Engineering

Discover

Review

From fundamental concepts to recent developments in the adhesive bonding technology: a general view

Catarina S. P. Borges[1] · Alireza Akhavan-Safar[1] · Panayiotis Tsokanas[1] · Ricardo J. C. Carbas[1] · Eduardo A. S. Marques[1,2] · Lucas F. M. da Silva[2]

Received: 4 April 2023 / Accepted: 4 May 2023
Published online: 25 May 2023

Abstract
Adhesive bonding is a constantly developing technique, and the volume of its industrial applications is rapidly increasing, which, in turn, requires improving the compatibility and performance of joining methods in specific applications. The industrial growth of adhesive bonding has also been linked to the broader implementation of composite materials and the increasing number of applications requiring joining dissimilar materials. Compared to traditional joining methods, adhesive bonding does not require local heating of the substrates or introducing holes or notches to them. It is instead a continuous joining method that promotes fewer regions of discontinuities and uniformity of the stress fields. Due to the industrial interest in this method, a substantial effort has been made to expand its range of applications and to provide the design tools that ensure it is a safe, reproducible, reliable, and durable process. The adhesive bonding research field is broad, ranging from adhesive formulation to evaluation of the final bonded structure. The present paper collects the relevant literature and discusses fundamental concepts and recent developments in the adhesive bonding technology, covering three essential topics: adhesive materials, joint designs and joint manufacturing methods, and joint modelling methods. Citing a wealth of relevant review papers, original papers, and book chapters, the paper intends to provide a coherent view of the state of the art, so the reader can identify the opportunities originating from the recent progresses in adhesive bonding.

Keywords Adhesive bonding · Adhesive materials · Design and manufacturing · Joint modelling · Overview

Abbreviations

CFA	Chemical foaming agent
CFRP	Carbon fibre-reinforced polymer
CZM	Cohesive zone model(ling)
DLJ	Double-lap joint
GFRP	Glass fibre-reinforced polymer
GSIF	Generalised stress intensity factor
PSA	Pressure-sensitive adhesive
SGA	Second-generation acrylic

✉ Eduardo A. S. Marques, emarques@fe.up.pt; Catarina S. P. Borges, cspborges@fe.up.pt; Alireza Akhavan-Safar, aakhavan-safar@inegi.up.pt; Panayiotis Tsokanas, panayiotis.tsokanas@gmail.com; Ricardo J. C. Carbas, rcarbas@fe.up.pt; Lucas F. M. da Silva, lucas@fe.up.pt | [1]Institute of Science and Innovation in Mechanical and Industrial Engineering (INEGI), Rua Dr. Roberto Frias, 4200-465 Porto, Portugal. [2]Departamento de Engenharia Mecânica, Faculdade de Engenharia, Universidade do Porto, Rua Dr. Roberto Frias, 4200-465 Porto, Portugal.

SLJ Single-lap joint
TEP Thermally expandable particle
TSL Traction–separation law
XFEM Extended finite element method
3-D Three-dimensional

1 Introduction

The adhesive bonding technique has been used for centuries by adapting natural materials to achieve a bond. Most materials historically used to adhere to others were obtained from natural sources, such as animal bones, plants, and minerals. However, about a century ago, synthetic adhesives have first been developed and implemented industrially [1]. Synthetic adhesives allowed for a much stronger adhesive bond, also enabling higher service life, with increased resistance to humidity and temperature. Among the first adhesives using synthetic materials are phenol–formaldehyde and urea–formaldehyde adhesives, which are still used to bond plywood. However, the first fully synthetic adhesive is phenol–formaldehyde, which was used for highly severe environments, such as waterproof plywood in boats. With research developments, acrylates were also introduced, followed by polyurethanes, swiftly expanding the range of adhesive applications. The creation of the epoxy adhesive has been pointed out as the biggest milestone in adhesive development over this time. The versatility and high mechanical properties of this material family have made it very popular in several industries, such as aerospace, automotive, naval, and construction [2].

These materials are often polymeric and have been presented as the 'diplomats' of the polymer class since they must have the ability to adhere to a wide variety of material families [3]. Nowadays, structures bonded with structural adhesives are seen as cost-effective and lightweight. Composite materials are often used in these applications since these materials allow for a high specific strength, decreasing structural weight. However, when composite parts are used, the method used to join them must be carefully selected, as composites are susceptible to notches and peeling loads. Methods that rely on the introduction of holes, such as riveting and bolting, must therefore be avoided since they can lead to the premature failure of the structure. Welding also has certain disadvantages since it does not work with thermoset-based composites and demands intense local heating of the material, which can introduce local damage and, consequently, a preferential failure path. As such, adhesive bonding is now seen as an emerging alternative for composite joining. Furthermore, it is advantageous for joining dissimilar adherends, including composites, metals, and polymers.

The present paper concerns the adhesive bonding technology in general, discussing both fundamental aspects and recent developments in it. Paper's focus in on adhesive materials, design and manufacturing methods (mainly for loading of the joint in shear), and modelling methods, with an emphasis on numerical modelling. The first section discusses the progresses in adhesive materials, divided into structural and non-structural adhesives, and highlights advances in second- and third-generation acrylics, toughened epoxies, and two-component polyurethanes for structural applications, and pressure-sensitive adhesives and bio-adhesives in the non-structural category. Afterwards, novel joint designs and manufacturing concepts are discussed, including functionally graded joints, hybrid joints, self-dismantling joints, and additive manufacturing applied to adhesive joints. The last section details joint modelling, covering the different numerical models and failure and life-prediction models. All sections start with highlighting the most important concepts, referencing review papers, book contributions, or original papers in the topic. Next, a handful of representative recent works are presented to emphasise recent trends. In our opinion, this structure makes it easier for the reader to understand the basic concepts of the different topics discussed and, at the same time, get informed about the most recent developments. Nevertheless, the great breadth of the topic under consideration has inevitably precluded us from providing a thorough review of the many and varied sub-topics discussed.

The remainder of this paper is organised as follows. Section 2 focuses on developments in the field of adhesive materials, discussing both structural and non-structural adhesives. Section 3 starts by discussing design options to optimise the properties of adhesive joints (namely functionally graded joints and hybrid joints). Next, developments in recyclability are comprehended through discussing self-dismantling joints, while the section closes by outlining recent developments in the additive manufacturing technique. Section 4 focuses on the modelling of adhesive joints and presents methods and models to predict the failure and the service life of joints. Finally, Sect. 5 concludes this paper.

2 Adhesive materials

Figure 1 classifies the adhesive materials into two major types: structural and non-structural adhesives. These two adhesive types can be further classified into more specific types, as shown in the figure. This section discusses these commonly used types of adhesive materials.

2.1 Structural adhesives

Structural adhesives have significantly evolved during the last decades, sustained by constant developments in the chemical science and engineering sector. While the first synthetic adhesives were mostly low-strength and brittle materials, modern structural adhesives can combine high strength and high stiffness with a satisfactory ductility. Among those adhesives, second- and third-generation acrylics, toughened epoxies, and two-component polyurethanes are the major adhesive types, and they are discussed below.

2.1.1 Second- and third-generation acrylics

Second-generation acrylics (SGAs) are acrylic adhesives first developed by DuPont (Wilmington, Delaware, USA). SGAs contain monofunctional methacrylic monomers or mixtures of (meth)acrylic monomers, elastomeric and polymeric thickeners, curing systems, and several modifying additives [4], usually in a two-component mixture. SGAs have satisfactory structural properties and cure rapidly at room temperature [5].

The two components contain one oxidant and one reducer, which, when mixing occurs, generate a chemical reaction that leads to the polymerisation of the acrylic material. The initial radical density does not affect the polymerisation, so these adhesives can cure using different mixing ratios, which offers varied mechanical properties [6]. Acrylic adhesives are known for their capability to adhere to different surfaces after minimal surface preparation and create high-quality bonds. In addition, SGAs are very versatile; they can be used both to fill a small gap in a structure and to repair damaged components in large-scale structures, such as in thick adhesive layers for the naval industry [7].

Recently, Sekiguchi et al. [5] studied the effects of loading rate and adhesive thickness on the fracture toughness of SGAs by using the double cantilever beam test. The fracture toughness was found to increase with increasing adhesive thickness, which was explained by the decreasing area of plastic deformation. SGAs whiten when plastically deformed, making it easier to identify the plasticised area. The authors reported that, for small adhesive thicknesses, the whole adhesive layer plasticised before failing, while, for larger adhesive thicknesses, plasticisation was localised.

Adhesive whitening can be explained by its modification using elastomeric spheres. These spheres increase the adhesive toughness, however, a phase separation with a sea–island structure occurs: the sea is an elastomer-rich zone, and

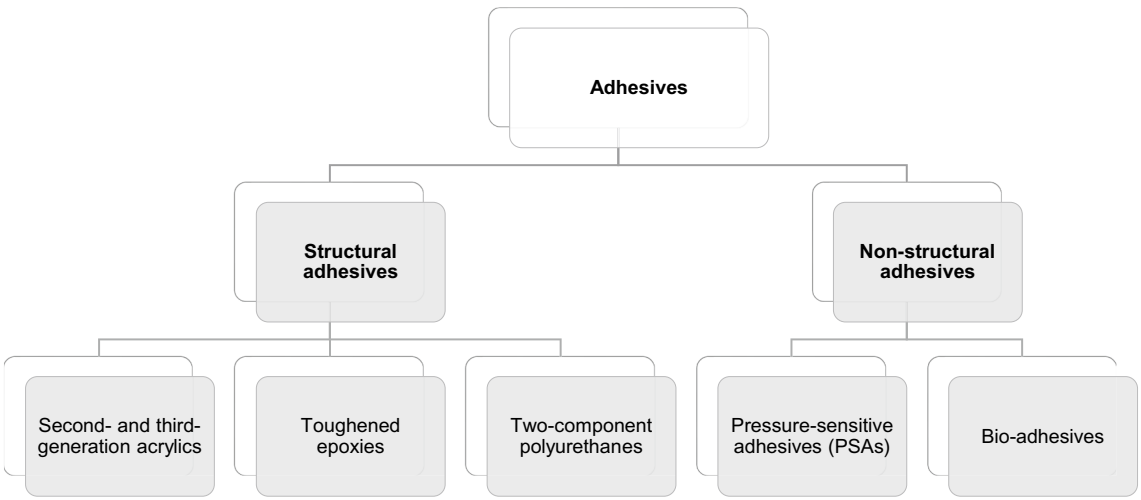

Fig. 1 A classification of the commonly used adhesive materials

the island is an acrylic-rich zone [8, 9]. Due to the stiffness difference between the sea and island zones, small cracks and cavities are formed in the adhesive when it is plastically deformed, leading to whitening and ductile failure.

In another recent work, Hayashi et al. [8] observed, using atomic force microscopy, the structures formed in the adhesive/adherend interface, employing SGAs and different plastic adherends. The sea–island structure formed was found to depend on the adherend material, and it could consist of either small islands (type 1) or large islands (type 2). In type 1, it was observed that there is a higher level of separation between acrylic particles and rubber, as for the islands in type 2, the acrylic resin is more uniformly distributed. Type 2 islands are stiffer and have a higher softening temperature, which leads to the conclusion that the rubber content of the island is lower than that of the sea. It was therefore concluded that this structure is influenced by the difference in rubber content ratio, and that adhesion and joint strength are both improved if the polymerisation of the acrylic resin leads to the formation of type 2 islands in the interface.

2.1.2 Toughened epoxies

Epoxies are perhaps the most prominent adhesive family that has been used in structural applications for more than 70 years [10]. They are thermosetting polymers, known for their high stiffness and strength, good adhesion properties, thermal stability, and high creep resistance. In contrast, among the main disadvantages of epoxies are their brittleness and low fracture energy [1, 11]. The brittleness of neat epoxy adhesives makes them inappropriate for several applications since they have a very small plastic deformation before failure. Additionally, epoxies do not have an adequate toughness for impact applications.

The principle for toughening an epoxy adhesive relies on increasing the ability of the material to dissipate energy using different deformation mechanisms [12]. Three main methods exist to toughen an epoxy adhesive: employing reactive oligomers; employing elastomeric particles; and employing other types of modifiers. The first method, which has been used for a longer period, consists of dissolving a reactive oligomer in the epoxy before applying the curing agent. As the curing process occurs, an elastomeric phase starts to precipitate, forming second-phase particles [13]. Following the second method, preformed particles are applied to the epoxy matrix [12, 13]. Following the third method, other types of particles are used to toughen the epoxy, such as alumina, silica, glass beads, and aluminium hydroxide [12].

Recently, the most used method is the second one. Developments have also been conducted on the particles used, evolving them to fillers with an elastomeric core and a thin glass shell, which are structured core–shell particles. The core of the particles is usually acrylic or butadiene. The elastomeric particles manufactured from these materials could stick together and introduce particle-rich and matrix-rich regions to the adhesive. Therefore, the main purpose of the shell is to help in handling the particles, making their distribution as uniform as possible. The shell must be designed to be compatible with each specific epoxy matrix considered [13]. The elastomeric particles used as toughers can reduce the strength, stiffness, and glass transition temperature, T_g, of the epoxy [12, 13]. However, these negative effects are compensated by increases in fracture toughness and impact properties of the material. Core–shell particles are responsible for the creation of internal cavities, and the elastomer cavitation is responsible for a decrease in the hydrostatic tension in the material, which finally leads to the initiation of a ductile shear yielding mechanism. Besides shear yielding, these particles can introduce additional toughening mechanisms, such as crack deflection, pinning, bridging or bifurcation, microcracking, and multilevel fracture paths [14].

The combination of elastomeric particles with other toughers is also under investigation. As an example, Kausar [11] investigated rubber-toughened, epoxy-based nanocomposites. Among the reinforcements investigated were graphene, carbon nanotubes, carbon black, and nanoclay. The first three reinforcements increased the fracture toughness of the rubber-reinforced epoxy, while the last one decreased it.

More generally, toughening of epoxy resins enables them to withstand loading conditions relevant to aerospace and automotive applications, which would be impossible using neat epoxy. Therefore, using different particle reinforcements and a combination of them in an epoxy matrix will certainly continue developing as a research topic.

2.1.3 Two-component polyurethanes

Polyurethanes can be thermoplastic, thermoset, or elastomeric polymers, and their properties can be tuned mechanically, thermally, or chemically [15]. Property tailoring can be achieved through the basic components—such as isocyanates prepolymers, polyoyls, functionality, and molar mass—and their formulation through component ratio for instance [16]. Therefore, the application range of polyurethanes is broad. For example, flexible foams are used in furniture, while rigid foams are used in medical applications and footwear. Moreover, polyurethanes are finding structural applications

in the automotive sector for plastic-to-metal or plastic-to-plastic bonding (e.g. bonding floors and vehicle windshields or interiors) [17].

The one-component polyurethanes cure by reaction with moisture, and carbon dioxide is released in this reaction. This phenomenon introduces porosities to the bond and renders it inappropriate for structural applications. In contrast, the two-component polyurethanes are modern adhesives used in structural joining applications, with high ductility and fracture toughness, and satisfactory damping, impact, and fatigue properties [18]. These materials can have different chemical structures, depending on the temperature of the chemical reactions and water in contact with the material during the manufacturing process. This water can be both in the environment and at the substrate surfaces [16]. If water does not come into contact with the material before the latter is cured (i.e. before the polyaddition of isocyanate and hydroxyl groups is complete), it will react with the isocyanate, which will later affect the curing reaction. For this reason, adhesive manufacturers often use formulations with an excess of isocyanate [19]. If water comes into contact with the material after curing, it can introduce moisture degradation, which is increasingly severe as temperature increases. Interestingly, Huacuja-Sánchez et al. [20] studied the effect of water on a two-component polyurethane and observed that, with water immersion, plasticisation of the material occurs, paired with decreases in the elastic modulus and the glass transition temperature, T_g.

Polyurethane adhesives are generally known to have large adhesive thicknesses in industrial applications, aiding in sealing and providing flexibility to the joint. The effect of adhesive thickness on the mechanical properties of two-component polyurethanes has been studied by Banea et al. [18]. The authors identified the critical adhesive thickness that leads to the maximum mode I fracture toughness and lap-shear strength. They also reported that, with increasing adhesive thickness, defects are more common, while joint's strength decreases, but this decrease is still lower than that for brittle adhesives.

The mode I crack growth behaviour of polyurethane adhesives was very recently studied by Ogawa et al. [21]. The authors found that, since these adhesives have high fracture toughness properties, the adherends of the joint may plastically deform. In such cases, adherend plasticity should be considered when determining the fracture toughness of the joint.

2.2 Non-structural adhesives

As with structural adhesives, non-structural adhesives have benefited from significant advances in chemical science and engineering, and multiple products using them have been developed for specific applications. There are two major families of non-structural adhesives: pressure-sensitive adhesives (PSAs) and bio-adhesives. Both these categories currently play important roles in bonded product design, and they are discussed below.

2.2.1 Pressure-sensitive adhesives (PSAs)

PSAs are viscoelastic materials that are permanently tacky in a solvent-free state and can adhere to surfaces under the application of low pressures [22, 23]. These adhesives do not rely on the curing of the material and can therefore be easily and safely applied at room temperature [23]. Using PSAs has been increasing in several industries due to their simple and clean bonding process, with easier handling, as well as the high strength without needing curing of fixtures. This makes these adhesives an appealing candidate for fast production cycles. These materials have been particularly growing in the electronic industry [24, 25]. Due to their simplicity and cleanliness, PSAs are highly relevant for industrial use, even if their performance is clearly non-structural. Bonding can be achieved through mechanical forces, chemical bonds, van der Waals forces, or moisture-aided diffusion of the adhesive into the substrate [26, 27].

PSAs are most commonly acrylics, silicones, or natural rubbers, and less commonly, polyurethanes, epoxies, or combinations of two or more materials [23, 28].

Acrylic PSAs have the qualities associated to acrylic adhesives, such as a high bondability to a wide variety of substrates [1], having the best balance of adhesion and cohesion. These materials are also highly transparent and non-yellowing, they have a low T_g, and they are resistant to solar radiation, oxidation, and water. Acrylic PSAs are used in tapes and labels, as well as in protective films. They are also very relevant in double-sided tapes, splicing tapes, protective foils, films, and medical products [23].

Silicone PSAs, as is the case with silicones more generally, are flexible adhesives with excellent resistance to environmental conditions (e.g. moisture, radiation) and to different chemicals [29]. These adhesives are also stable in a wide range of temperatures (usually up to 250 °C) and compatible with several different surfaces [30]. Silicone PSAs

are used in tapes, labels, electronics, and medical applications [23]. The latter is among the most essential applications for these materials, due to their biocompatibility, both in wound management, transdermal drug delivery systems, and bio-devices.

Natural-rubber PSAs usually refer to cis-1,4-polyisoprene—which is obtained from trees and plants—and have the ability of crystalising under stretching. Such adhesives are used in several PSA applications, given that cis-1,4-polyisoprene is the most common base for elastomeric PSAs. However, these materials do not present the required adhesion and tack properties by themselves. Therefore, using fillers is typically required to achieve those appropriate properties for specific applications, turning the natural rubber into a PSA. Tackifier resins can be aliphatic or aromatic hydrocarbons, polyterpenes, or rosin derivatives [31].

Recently, Chung and Kwak [32] evaluated the shock absorption and strength under shear impact for different adhesives, one of which was foam tape. This material revealed a superior performance in terms of shock absorption and was recommended for mobile electronic applications, when compared to liquid bonds cured using ultraviolet. The authors also mentioned that this material would be more reliable for battery applications than for glass window applications.

In another recent work, Son et al. [33] studied PSAs used in temporary pavement marking, which, if peeled off, can lead to automotive accidents. Understanding how adhesive properties change with environmental conditions (e.g. temperature, humidity) is essential for this application. To this end, the materials were analysed by the authors from −20 to 40 °C. The peel load decreased as the temperature increased, and at −20 °C, the temperature was lower than the T_g of the top layer, leading to a brittle failure.

2.2.2 Bio-adhesives

Most adhesives used in industrial applications are petroleum-based products, which comes associated with major environmental and economic disadvantages. From an environmental point of view, fossil-based products are known to have an impact on the soils, air, water, and on living species. From an economic point of view, due to the unpredictability of the petrochemical industry, the price of petroleum is also unstable, which can lead to changes in the cost of the adhesive itself [34]. Therefore, natural materials have been adapted recently to be used in these applications and are being modified to improve their bondability and mechanical properties, while retaining a low cost.

Many bio-adhesives have been formulated to be used with wooden substrates for structural applications. Apart from the economic and environmental benefits, the main purpose of these materials is to substitute adhesives with formaldehyde [35] since, in 2008, the Environmental Protection Agency classified formaldehyde as carcinogenic, and it is progressively being removed from commercial products [36].

For applications with wood or other substrates, the main natural materials used as synthetic adhesive substitutes are lignin, tannin, carbohydrates, unsaturated oils, proteins, and their derivatives:

- Lignin is one of the most abundant compounds in biomass, following cellulose and hemicellulose, all of which are found in trees and plants [36]. It is a phenolic material and the main by-product of the paper pulping industry [37]. Lignin is mainly used incorporated into phenolic adhesives, such as urea formaldehyde and phenol–formaldehyde [38]. Promising results have been reached with lignin from softwood, and kraft lignin was found to have the best compatibility to replace phenol. This, however, comes with the disadvantage of increasing pressing time [39]. To solve this problem, it is proposed that the lignin should pre-react with formaldehyde and only then be added to the phenol–formaldehyde resin [40].
- Tannin is traditionally used in the leather industry to turn hide into leather, while it has been used as a bio-adhesive for more than four decades [41]. This material can be found in the soft tissue of trees and is generally used to substitute phenol. Condensed tannin represents most of the tannin production and can be hardened for adhesive use through self-condensation or using a hexamethylene hardener. Both techniques are under consideration for industrial use [42].
- Carbohydrates, such as starch, cellulose, and hemicellulose, can also be used to formulate bio-adhesives. Starch has acceptable adhesion and film formation properties but is prone to hydrogen bonds and, therefore, has low durability in humid environments [41].
- Other bio-adhesives, such as protein-based or casein-based ones, can also be used. Among them, soy-based adhesive should be highlighted since it has been used with promising results [43].

Although bio-adhesives provide constantly improving mechanical behaviour and applicability, durability is still a concern since these materials degrade under severe environmental conditions, which is not desirable for many structural applications. A very recent review on bio-adhesives and their use in wooden adhesive joints can be found in Ref. [44].

3 Design and manufacturing methods

Design and manufacturing of bonded joints is a broad and essential topic in adhesive bonding. Joint design should be carefully adjusted to match the loading and service conditions, while it aims at the optimal exploitation of adhesive and adherend properties. Several designs have been proposed in the last decades, seeking to improve joint performance and manufacturability. Some proposed design and manufacturing methods have been proven especially promising, so they have been the target of focused research in the last few years. These methods include functionally graded joints, hybrid joints, self-dismantling joints, and additive manufacturing in joint design (see also Fig. 2), all of which are discussed below.

3.1 Functionally graded joints

The adhesive joints are designed so that the adhesive is loaded in shear whenever possible, aiming to increase the resistant area and, thus, the joint strength [1]. The most typical case of joint following this design rationale is the single-lap joint (SLJ) (Fig. 3a). As loading is applied to this joint, the vectors of the two forces tend to coincide, so the ends of the

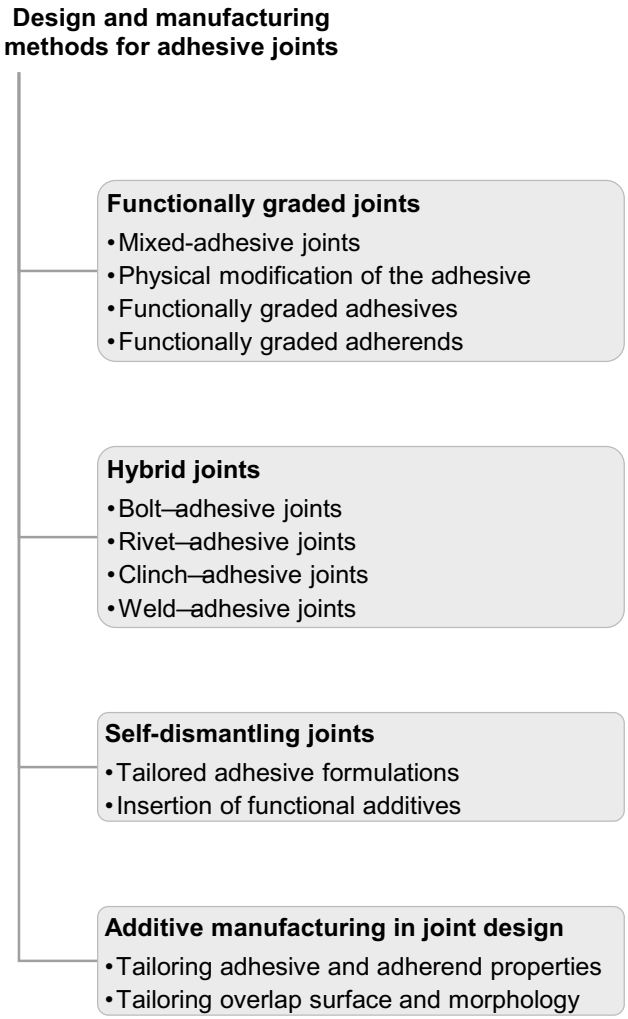

Fig. 2 A broad classification of promising methods for the design and manufacturing of adhesive joints

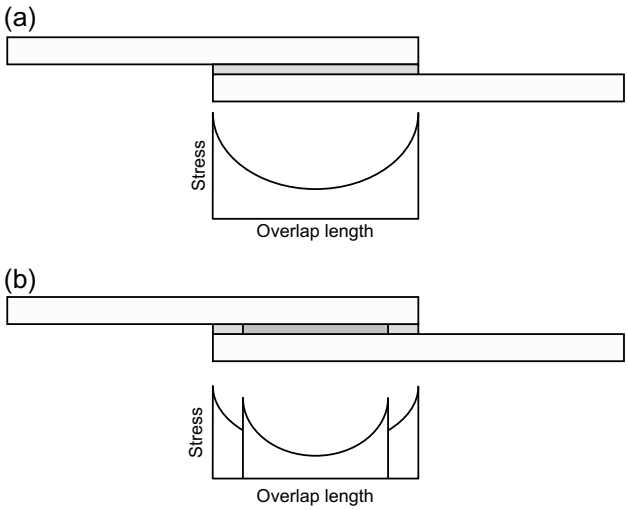

Fig. 3 Shear stress distribution in a SLJ using **a** a single adhesive and **b** a mixed-adhesive technique employing two adhesives (adapted from [49])

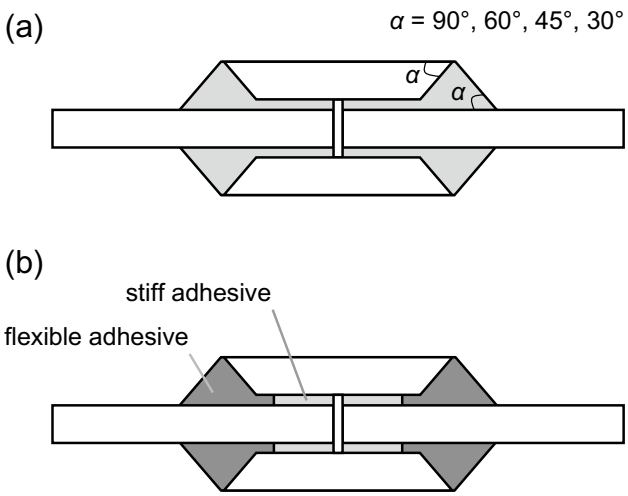

Fig. 4 Tapered adhesive joint with **a** a single adhesive and **b** mixed adhesives, as proposed by Marques and da Silva [52]

overlap are loaded in bending. As a result, the developed shear stress in the bondline is not uniform along the overlap length but shows a minimum in the middle of the overlap and a maximum at its ends (see Fig. 3a).

Different designs have been proposed to maintain as uniform stress distribution as possible and thus increase joint strength, particularly when high-stiffness adhesives are used. Raphael [45] was the first to propose the concept of graded adhesive joints by employing a more flexible adhesive at the overlap ends and stiffer adhesives closer to the overlap middle. This concept was first studied numerically by Hart-Smith [46], and it then evolved towards mixed-adhesive joints, physical modifications of the adhesives, functionally graded adhesives, and functionally graded adherends.

3.1.1 Mixed-adhesive joints

As mentioned, the mixed-adhesive method proposes a bondline with adhesives of increasing stiffness from the ends to the middle of the overlap [45]. Pires et al. [47] tested this method using aluminium adherends and found that it can increase joint strength. Fitton and Broughton [48] employed carbon fibre-reinforced polymer (CFRP) and steel-to-CFRP adherends. The method proved capable of reducing the peel loading and shear stress concentrations, which increases joint strength. da Silva and Lopes [49] studied a two-adhesive joint, keeping fixed the brittle adhesive in the overlap middle and changing the ductile adhesives at the overlap ends. Using mixed adhesives resulted in a higher failure load when compared to using the brittle adhesive alone, regardless of the type of the ductile adhesive used. Although the average stress was improved, there were still areas of stress concentrations, as shown in Fig. 3b.

Temiz [50] applied the method to double-lap joints (DLJs) and showed that the method is useful for decreasing the stress concentration at the ends of the overlap. das Neves et al. [51] analytically modelled mixed-adhesive SLJs and DLJs

with two adhesives along the overlap, tested at different temperatures. This model can be used to determine the best combination of adhesive properties and the joint geometry that achieve the optimum joint behaviour.

Marques and da Silva [52] extended the mixed-adhesive method to joints with an internal taper and a fillet, as shown in Fig. 4. The influences of taper angle and mixed adhesives on the shear strength of the joint were analysed. It was found that tapered patches have a significant influence only when stiff adhesives are used, leading to a joint strength increase of up to 30%. It was also found that a 45° taper angle reduces stresses at the ends of the overlap. The combination of ductile and brittle adhesives proved to have a synergistic effect in configurations without a taper. However, the failure loads of the joints with only the stiff adhesive and those with mixed adhesives were comparable, while mixed-adhesive joints have the extra advantage of being more ductile and flexible.

In the mixed-adhesive method, it should be ensured that the adhesives are chemically and mechanically compatible, and that their curing cycles can be matched. Among the main issues with this method is the proper separation of the two (or more) adhesives. Marques and da Silva [52] proposed separating the adhesives using silicone strips. The best way to control this process would be using only film adhesives; it is however difficult to find film adhesives with compatible properties and curing characteristics.

The mixed-adhesive joints should be studied at different temperatures to ensure that the thermal expansion coefficients—and thermal properties, in general—of the adhesives are compatible. Hart-Smith [46] was the first to investigate mixed-adhesive joints at both high and low temperatures. He concluded that, at low temperatures, the low-temperature adhesive (usually the ductile one) transfers the entire load, while at high temperatures, the high-temperature adhesive (usually the brittle or stiff one) is the load-bearing material. da Silva and Adams [53] experimentally studied mixed adhesives in joints that must withstand extreme (either high or low) temperatures. The authors concluded that the concept is useful on epoxy mixed-adhesive joints under quasi-static loading, particularly if dissimilar adherends are considered.

Recent developments in mixed-adhesive joints have been made thanks to novel adhesives, such as SGAs. Based on the fact that the properties of SGAs can change by changing the mixing ratio of the reactants in the curing of the adhesive, Sekiguchi et al. [5] created a mixed-adhesive joint, where the adhesive properties changed stepwise along the overlap by changing the amount of the stiff agent (Fig. 5). The strength of the mixed-adhesive joint was greater than that of the stiff and flexible adhesives, with the strain at the overlap ends being decreased by 40% when compared to the joint with only the flexible adhesive. Additionally, the mixed-adhesive joint behaved better than the others for low-cycle tests, increasing by more than four times the fatigue life.

3.1.2 Physical modification of the adhesive

Varying properties along the overlap of the joint can be achieved not only using different adhesives or adhesives with different compositions but also using local reinforcements to the adhesive.

As an example, Sancaktar and Kumar [54] added rubber particles in the areas near the ends of the overlap and achieved increases in the fracture toughness of the adhesive and in the joint strength. It was found that, for a given particle volume fraction, the smaller the particles, the higher the toughness of the adhesive. This trend is only valid until a certain particle size, from which the particles are so small that their effect becomes negligible. Therefore, it becomes clear that an optimum particle size exists that maximises fracture toughness [55].

Stapleton et al. [56] strategically placed glass beads along the overlap to change the adhesive thickness. With this method, the authors achieved a reduction of the peel stresses. However, this technique did not ensure a uniform stress distribution along the overlap width. To overcome this issue, Silva et al. [57] reinforced an epoxy adhesive using cork

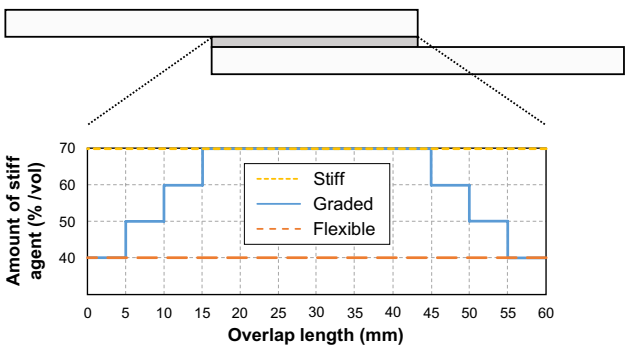

Fig. 5 Stiff agent distribution of mixed-adhesive SLJ with an SGA (adapted from [5])

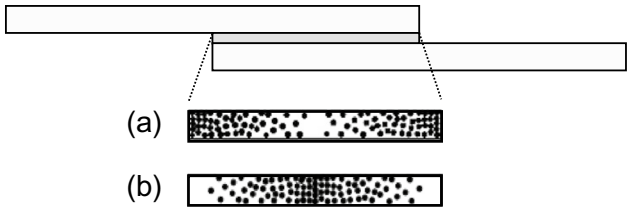

Fig. 6 Reinforcement of the adhesive by adding particles: **a** addition of cork particles to an epoxy adhesive; **b** addition of iron particles to a polyurethane adhesive

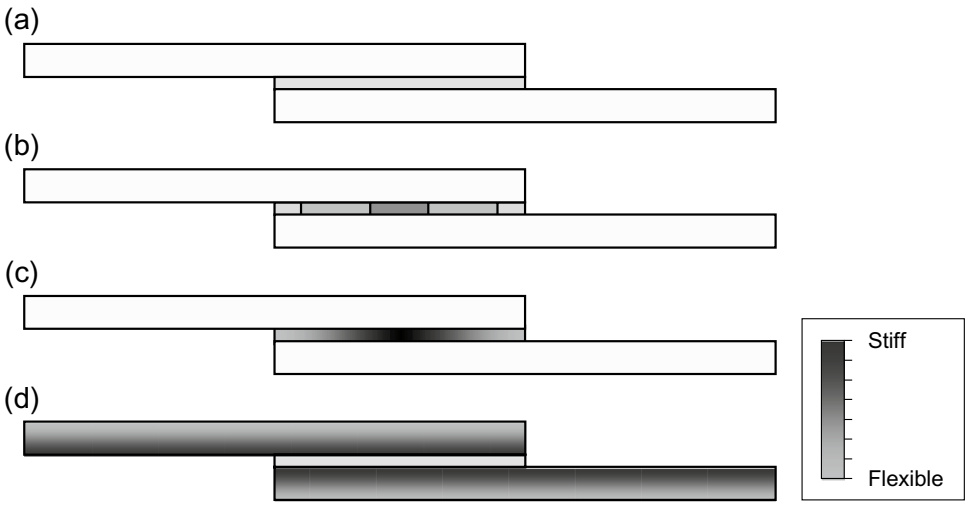

Fig. 7 **a** Adhesive joint; **b** mixed-adhesive joint; **c** adhesive joint with functionally graded adhesive; and **d** adhesive joint with functionally graded adherends (as presented by Chen et al. [73])

particles with a metallic coating that provided them with magnetic properties. With an array of magnets placed in critical positions outside the mould where the SLJs were manufactured, the authors achieved to move the particles and place them in a gradient along the overlap (Fig. 6a). The same rationale was applied in the opposite way in Ref. [58], where a polyurethane adhesive was reinforced using stiff iron particles (Fig. 6b).

3.1.3 Functionally graded adhesives

The previous two methods allow for a stepwise variation of the adhesive properties along the overlap (Fig. 7a, b). Functionally graded adhesives can however be obtained by continuously changing material composition or microstructure along the overlap length (see Fig. 7c). Practical methods to obtain functionally graded adhesives include the following two: mixing adhesives with particles of different properties or in different volumetric percentages to create a non-uniform reinforcement distribution in the bondline; and applying different localised curing cycles. Compared to the stepwise variation of adhesive properties, the functionally graded adhesives allow for a much more uniform stress distribution in the bondline and reduced peel stresses at the overlap ends.

Kumar [59] performed a theoretical analysis of tubular joints with different stiffnesses along the bondline, using a continuous variation in modulus through a quadratic function and a discrete stepwise approximation of that function, as with mixed-adhesive joints. It was seen that the functionally graded joint exhibited smaller shear and peel stresses. Kumar and Scanlan [60] continued Kumar's work by proposing a model for the prediction of the stress distribution in a functionally graded joint. This model was used to predict the normal stress in stiff joints and the loss of stiffness at the interface due to previous defects and damage.

Carbas et al. [61] extended this study for SLJs by developing a theoretical model based on Volkersen's analysis and using a power series expansion. The authors validated their model against a finite element analysis. Similarly to Kumar [59], Carbas et al. showed that the functionally graded joints are stronger than the respective baseline joints (without grading). It was also concluded that the effectiveness of this procedure was higher as the overlap length was increased.

Carbas et al. [62] proposed an SLJ with a functionally graded adhesive based on a graded curing of the adhesive by induction heating, which leads to a graded stiffness: maximum in the middle of the overlap and a minimum at its ends. A 60% increase in joint performance was achieved as a result. The same joints were then subjected to post-curing [63]. It was found that, for post-curing at a lower temperature than the T_g, the strength of the graded joints slightly decreases

while for post-curing temperatures above the T_g, the graded joint behaviour was similar to that of the evenly cured joints. Carbas et al. [64] used this concept to improve the performance of wooden specimens repaired with CFRP patches.

Kawasaki et al. [65] used a mixture of a brittle and a flexible SGA and applied different mixing ratios. These mixing ratios were evaluated based on tensile tests, while the hardness of the adhesive was evaluated through nano-indentation in key locations of the manufactured joint. The hardness evaluation verified that the intended gradient of properties had been achieved, while the hardness showed a variation with the mixing ratio and Young's modulus.

3.1.4 Functionally graded adherends

Another method to decrease stress concentrations at the overlap ends is using functionally graded adherends (see Fig. 7d). At the same time, this technique can be used to improve other physical properties of the joint, such as thermal and electrical conductivities [66]. The concept of functionally graded adherends has been introduced two decades ago by Ganesh and Choo [67]. This concept is generally considered effective, but it usually requires a complex manufacturing process, so the existing literature consists mainly of numerical and analytical studies. Different techniques have been investigated towards developing a graded adherend stiffness, two of which are discussed below [66]: braided fibre angles [67, 68] and graded metal–ceramic layers [69, 70].

Uniformly braided fibres (i.e. three or more yarns intertwined, so no two yarns are twisted around one another) and fibres with graded angles, which lead to a graded adherend stiffness, have been investigated by Ganesh and Choo [67] and Boss et al. [68]. Several distributions were compared, including linear and parabolic. This technique was compared to geometrically graded adherends, and the latter led to a more effective reduction of stress concentrations. A functionally graded stiffness was also achieved using metal–ceramic adherends.

A few experimental studies are available in the literature. Melograna and Grenestedt [71] attempted to create a stiffness gradient along the adherend length by introducing holes with progressively smaller diameters, starting from the end of the adherend and along the overlap. The variables of their study were the adherend thickness, width, and length, as well as perforation shape, size, and distribution laws. As a result, the optimum joint configuration was determined based on the maximum failure load. Specifically, the optimum configuration was that with 7–9 rows of graded perforations, triangular or circular. More recently, Kumar and Tejada Alvarez [72] employed a variable-thickness (tapered) adherend. The adherends were manufactured using three-dimensional (3-D) printing, which allowed higher design flexibility. All graded joint configurations exhibited an increase in joint strength when compared to the standard joint, and the best configuration achieved an 80% increase in the failure load.

Recently, Chen et al. [73] performed a numerical analysis of the stress distribution of SLJs with graded adherends. The failure behaviour of the joint was studied through cohesive zone modelling (CZM). In addition, the properties of a brittle and a ductile adhesive were used in the overlap. It was shown that the brittle adhesive is more sensitive to the gradation of mechanical properties along the overlap since it is less able to redistribute stresses along the overlap.

3.2 Hybrid joints

The basic types of hybrid adhesive joints, which combine adhesive with mechanical joining, are four: bolt–adhesive joints, rivet–adhesive joints, clinch–adhesive joints, and weld–adhesive joints [74].

3.2.1 Bolt–adhesive joints

The bolt–adhesive joints, also widely referred to as bolted–bonded joints, constitute the most common type of hybrid adhesive joints. Figure 8a illustrates a typical bolt–adhesive joint between aluminium and glass fibre-reinforced polymer (GFRP). In such joints, the bolts do not significantly contribute to load transfer until failure initiation but contribute to reducing the stresses at the overlap end, especially after failure initiation.

Caccese et al. [75] experimentally evaluated the influence of stress relaxation on clamp-up load in composite-to-metal bolt–adhesive joints, showing that the most significant factor in the clamp-up load loss are the thermal effects. Matsuzaki et al. [76] proposed a hybrid joining method that combines co-cured adhesive joints and bolted joints, without damaging the reinforcing fibres. The study showed that the hybrid joint has a 1.84-times-higher maximum shear strength than the conventional co-cured joint and much higher fatigue strength than the bolted joint. Barut and Madenci [77] developed a semi-analytical solution method for stress analysis of bolt–adhesive SLJs between composite laminates under general

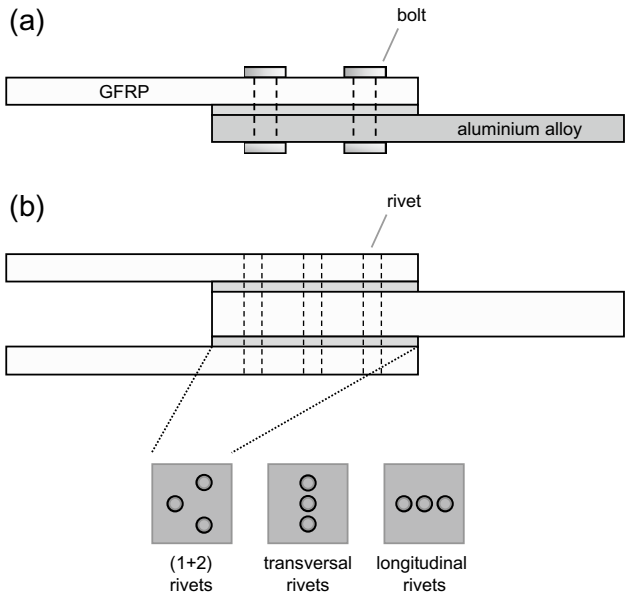

Fig. 8 **a** A bolted/co-cured joint between GFRP and aluminium [76]. **b** A rivet–adhesive DLJ and three typical rivet arrangements [83]

loading. This method allows for the determination of pointwise variation of displacement and stress components and the bolt load distribution.

Very recently, Boretzki and Albiez [78] studied the influence of adhesive stiffness on bolt–adhesive joints, concluding that high-stiffness adhesives are required to increase the load-bearing capacity of the joint. Delzendehrooy et al. [79] studied the mechanical behaviour of bolt–adhesive SLJs subjected to ageing. Increasing bolt sizes for the same overlap region led to a higher failure load. However, the higher the diameter-to-width ratio of the hole, the more extensive the adhesive failure observed in the aged conditions.

3.2.2 Rivet–adhesive joints

Figure 8b schematically represents a rivet–adhesive DLJ and three characteristic rivet arrangements. As explained below, rivet arrangement is a key factor in the mechanical behaviour of the joint.

Pirondi and Moroni [80] studied the failure behaviour of rivet–adhesive joints for different damage models. It was shown that the adhesive layer strongly increases the initial stiffness and maximum load of the rivet–adhesive joints compared to a pure-rivet joint.

Sadowski and co-workers numerically and experimentally investigated rivet–adhesive DLJs using steel [81] or aluminium [82] adherends. It was found that the tensile strength of the adhesive joints with single or multiple rivets was higher than that of the pure-adhesive or pure-rivet joints. In addition, the hybrid joints showed a significant energy absorption capacity when compared to the pure-adhesive joint. Next, Sadowski and Zarzeka-Raczkowska [83] studied the influence of the rivet arrangement (see Fig. 8b) on the strength of aluminium DLJs. The '1 + 2 rivets' arrangement showed the best performance, characterised by the most regular strain distribution around the rivets and the highest energy absorption.

Solmaz and Topkaya [84] studied composite rivet–adhesive DLJs for different overlap lengths. For all overlap lengths studied, the hybrid joints showed the highest strength compared to the pure-adhesive and pure-rivet joints. Increasing the overlap length led to a similar failure load value between the hybrid joint and the purely riveted joint.

Liu et al. [85] proposed the single-sided piercing riveting technique to join two or more sheet parts. This technique was compared with other joining techniques and showed superior performance against riveting. Next, Fiore et al. [86] investigated the effect of curing time on the performances of hybrid joints with dissimilar adherends. The self-piercing riveting technique was applied to joining aluminium with GFRP adherends. The authors evaluated the influence of the curing time of the epoxy resin used in the composite and in the bonded area. It was shown that when an adhesive/self-piercing riveting hybrid joint is manufactured, the timing when the rivet is inserted during the adhesive bonding process is a critical parameter of the joint performance.

Recently, Jiang et al. [87] stated that using adhesive can prevent the appearance of corrosion products in the clearance, but it increases the joint vulnerability to chloride ions damage, affecting corrosion resistance for long exposure times.

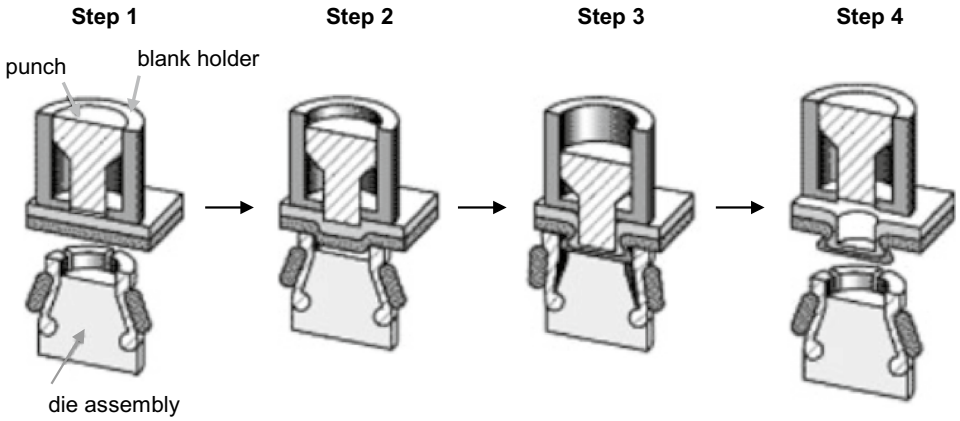

Fig. 9 A schematic of the clinch joining process (taken from [74])

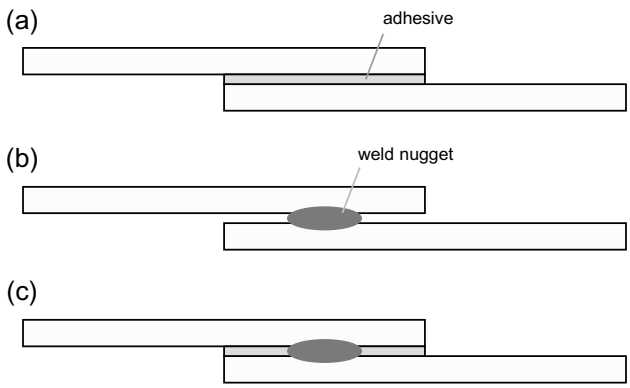

Fig. 10 An adhesive joint **a**, weld joint **b**, and weld–adhesive joint **c**

This damage is minimised when rivet–adhesive joints are used. Ibrahim and Cronin [88] tested adhesive, self-piercing riveted, and hybrid H-shaped tension specimens. The energy absorption was found to increase in the hybrid joints when compared to both adhesive and riveted joints, without compromising strength and stiffness for sheets with thicknesses of 1 and 2 mm.

3.2.3 Clinch–adhesive joints

Clinching, or press joining, is a mechanical fastening technique for point joining of sheet metals, which can be used for a sheet with a 0.5 to 3 mm thickness, so the total joint thickness can be up to 6 mm. The clinch joining process consists of the following four steps (see Fig. 9) [74]: in step 1, the sheets are clamped between a die and a blank holder; in step 2, the punch locally pushes the sheets down into the die; in step 3, the sheets are squeezed between the punch and die, expelling material sideways; and in step 4, an interlocking button is formed.

Pirondi and Moroni [80] numerically studied the failure behaviours of rivet–adhesive and clinch–adhesive joints. The authors concluded that the different damage models with experiments performed on simple joints can be combined in a unique model to effectively simulate the failure behaviour of clinch–adhesive joints. Balawender et al. [89] studied numerically and experimentally the behaviour of clinch–adhesive joints subjected to tensile loading. Two procedures were employed to manufacture the hybrid joints: adhesive curing before clinching and clinching before adhesive curing. The second manufacturing procedure created stiffer hybrid joints up to the maximum force, although the first manufacturing procedure showed higher separation force, joint strength, and energy absorption.

More recently, Moroni [90] studied the static and fatigue behaviour of clinch–adhesive joints, self-piercing rivet–adhesive joints, and purely adhesive joints, always using aluminium adherends. Both hybrid joints showed worse fatigue behaviours than the purely adhesive joints at low numbers of cycles but better behaviours at higher numbers of cycles. Moreover, mechanical fastening decreased the crack growth rate in the adhesive layer of both hybrid joints, thus extending the joint's fatigue life. Zhuang et al. [91] studied the effect of the curing degree of an epoxy adhesive used in a clinch–adhesive joint between aluminium and steel alloys. Interestingly, the uncured adhesive showed the highest mechanical performance, which showed a decreasing trend with increasing curing degree.

3.2.4 Weld–adhesive joints

Figure 10 schematically compares an adhesive joint, a weld joint (using spot-welding), and a weld–adhesive joint.

Moroni et al. [92] experimentally analysed the strength of adhesive joints, spot-welded joints, and weld–adhesive joints. The weld–adhesive joints showed increased stiffness, strength, and energy absorption compared to the spot-welded joints, as well as a reduced dependency on temperature and ageing compared to the adhesive joints.

Campilho et al. [93] performed an optimisation study of weld–adhesive SLJs. The authors showed that, for small overlap lengths (15 mm), the strength of the weld–adhesive joint is 24% higher than that of the adhesive or spot-welded joints. For larger overlap lengths (60 mm), this strength became 1.8% higher than the adhesive joint and 58% higher than the spot-welded joint.

Very recently, Wang et al. [94] used a combination of friction stir welding and an epoxy adhesive bonding for aluminium alloy joining. It was observed that adding the adhesive does not cause premature cracking since its elastic limit is higher than that of the conventional joint. It was also shown that the transition zone decreases stresses and contributes to a more uniform stress distribution, also blocking the corrosion media.

3.3 Self-dismantling joints

Some materials commonly used in adhesive joints, such as CFRPs and ceramics, are usually expensive and might affect the environment once they become useless. In the automotive industry, for example, recycling, recovery, and reuse of end-of-life vehicles have raised world concerns. The production of vehicles in some countries has overcome the capacity of the recycling industry to process them when they are no longer operating. Typically, end-of-life vehicles are either scrapped for recycling or simply abandoned on the road. However, abandoned vehicles cause obstruction and safety problems in public place, as well as waste resources [95].

For these economic and environmental reasons, developing new technologies and processes for easy recycling and repairing of bonded structures is becoming essential in several industrial sectors. A major problem in recycling adhesive joints appears when the adherends must be disassembled without being damaged so that they can be reused. A handful of conventional techniques for adhesive dismantling is still commonly used for adhesives that have not been modified prior to bonding. Mechanical separation is the earliest method, generally inefficient and laborious due to the lack of clean separation of the adherends, although some patented work has attempted to ease this process. Another conventional technique is through heating the adhesive until it reaches a temperature above its T_g, where it becomes softer, or through exceeding the temperature of flammability-in-air or auto-ignition point to achieve a thermal decomposition. The main disadvantages here are the cost of reaching these temperatures and the emission of toxic and irritant gases because of chemical decomposition. A third conventional dismantling technique is through immersion of the joint in solvent or acid. Isopropyl alcohol, methyl ethyl ketone, and acetone are some effective polar solvents for cleaning and degreasing substrate surfaces [95].

Below, we discuss innovative techniques for adhesive disassembly. Two main routes have been identified: tailored adhesive formulations, based on the modification of the adhesive formula to ease disassembling; and inserting functional additives to trigger the debonding process.

3.3.1 Tailored adhesive formulations

Battelle Memorial Institute performed one of the first attempts to obtain easy adhesive disassembly through changing the original chemistry formula of the adhesive [96]. A thermally reversible isocyanate-based polymer formulation was developed, and its mechanism was based on the dissociation of the isocyanate-labile hydrogen-based linkage to the isocyanate and labile-hydrogen starting groups. However, this system was found to become a free-flowing melt, which was soluble in acids.

Sandia National Laboratories modified a low-modulus epoxy adhesive by incorporating furan maleimide Diels–Alder adducts to create a thermally removable adhesive. These adducts form below 60 °C and dissociate above 90 °C. In this case, experimental tests showed poor lap-shear strengths, making the adhesive unsuitable for structural and other applications due to its low dissociation temperature.

EIC Laboratories created the ElectRelease™ innovative system to electrically disbond adhesive joints [97]. With this technology, joints bonded with structural epoxy adhesives can be easily dismantled by just applying a current of 10–50 V. The debonding needs a metal as the positive substrate and another suitable material as the negative substrate, and it is

achieved by ion conduction along the resin/metal interface. Joint surfaces must be electrically conductive, while kissing bonds must be avoided to prevent any short circuit between substrates [97]. This technology can be applied to non-conductive or coated substrates using an aluminium foil patch, prebonded with ElectRelease™.

Motivated by the ElectRelease™ technology, additional investigations were performed to disbond adhesive formulations. For example, a delamination process at the interface between the aluminium anode and the adhesive layer was observed in Ref. [98]. The changes in polymer chemistry were detected using Raman spectroscopy, and the emission of volatile species was analysed using mass spectrometry.

Dismantling and recyclability of thermoset adhesives are also under study. Very recently, Santiago et al. [99] prepared a series of epoxy-based vitrimers that showed good thermomechanical properties and the possibility to create adhesive joints capable of being dismantled and re-joined.

3.3.2 Insertion of functional additives

Several studies and patents have been developed on the incorporation of additives into the adhesive to assist the debonding process. Chemical foaming agents (CFAs) and thermally expandable particles (TEPs) are the two additive types that stand out nowadays.

CFAs are added to the adhesive to ease the disassembling process at high temperatures. A series of CFAs have been investigated by Henkel, IBM, US Army Research Laboratory, and Rescoll, including Azo compounds and hydrazides. At high temperatures where the adhesive bondline softens and melts, CFA additives would mobilise, and some of them migrate and decompose at the joint interface [95].

TEPs are made of a thermoplastic shell filled with liquid hydrocarbon. The system experiences two transformations when heated [100]: firstly, the shell material becomes softer; and secondly, the hydrocarbon liquid inside changes into a gas state. As a result, the spherical particle expands until it reaches a volume from 50 to 100 times the initial one. Once heating stops, the sphere stiffens and remains expanded.

In Ref. [101], the TEP technology was applied to structural adhesive bonding for recycling purposes. When applying temperatures higher than 100 °C, the expansion of the particles inside the adhesive significantly eases the separation of the adherends (Fig. 11). According to this study, the expansion of the adhesive can be up to 400% of the initial volume. The main disadvantage observed was that the adhesive started to expand over 60 °C, and its T_g was below the expansion temperature of the particles, which limits the adhesive's application in demanding industrial sectors, such as automotive.

Additionally, the water uptake percentage of the adhesive increases with TEP content, decreasing the long-term stiffness and strength of the structure [102]. Interestingly, TEPs have recently been proposed as a means to combine self-dismantling and functionally graded properties along the adhesive, as they showed an increase in the fracture toughness of a polyurethane adhesive [103].

It is noted that none of the two approaches mentioned above creates a system sufficiently effective for the disassembly of an adhesive applied in the automotive industry. Disassembly efficiency and additive–matrix compatibility were identified to be two major concerns, which were either vaguely mentioned or completely neglected in most patented works. Although some studies have highlighted these two major concerns, there are currently no feasible solutions [95].

Additional techniques have been developed to assist the dismantling of adhesive joints without significantly affecting adhesive properties. Introducing carbon nanotubes into a conventional epoxy has been shown to enhance its thermal conductivity, heat resistance, mechanical properties, and long-term durability. Likewise, introducing graphene into the adhesive can enhance it to a comparable level and at a lower cost. It is believed that the increase of thermal conductivity by incorporating these elements could enhance the disassembly efficiency, as heat is transferred to functional additives much faster [95]. Micro-patterned carbon nanotube-based tapes have been developed [104] and formed the basis of a new adhesive class that adapts to a continuous bonding and debonding process.

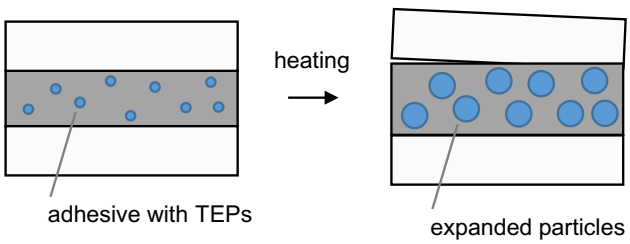

Fig. 11 Mechanism of debonding in an adhesive with TEPs (adapted from [100])

3.4 Additive manufacturing in joint design

A significant industrial interest in additive manufacturing has been shown in recent decades. Consequently, modern 3-D printing machines [105] with novel features, such as multimaterial additive manufacturing simultaneous processing [106], have been developed. The same industrial interest has led to the adoption of new approaches to design for additive manufacturing [107] with new materials and to an increased process standardisation [108]. Many studies have demonstrated how positioning for printability, printing setups, and printing parameters can affect the surface finishing, geometrical accuracy, and mechanical properties of the resulting components [107, 109]. These issues are covered in our recent review in Ref. [110].

The process of optimising the design of bonded joints can be seen as a maximisation process of the load-bearing capacity of the assembled components. Joint design strategies were initially based on selecting materials with enhanced material properties and maximising the bonding area. Later, the growing need for lightweight structures, the investigations on the physics of adhesion, and the advances in modelling techniques laid the foundation for alternative joint design strategies. These include tailoring adhesive and adherend properties and tailoring overlap surface and morphology [111].

3.4.1 Tailoring adhesive and adherend properties

Additive manufacturing has been used to locally change the material properties in the joint. This can be implemented by simultaneous deposition of different materials (for example, with multimaterial additive manufacturing [106]) to obtain functionally graded adherends or adhesives. This design concept has already been investigated for other manufacturing processes [68, 112]. Alternatively, additive manufacturing can be used to create complex structures in the thickness direction, such as lattice, cellular, or auxetic structures. These structures introduce tailored porosity, macro-voids, or cavities into the adherends, increasing the stiffness of the joint.

Additive manufacturing enables control over the material at voxel resolution, which, if coupled with multimaterial additive manufacturing, can be used to create joints whose adhesives have tailored physical and mechanical properties. Among the main engineering challenges in tailoring adhesives is to obtain a seamless variation in the material properties (i.e. functionally graded adhesive behaviour; see Sect. 3.1.3) [112].

3.4.2 Tailoring overlap surface and morphology

Adhesion mechanisms can be described using three classical theories [113]. The first one is the absorption theory, which describes the forces of attraction (primary bonds, such as covalent, or van der Waals forces) acting between the adhesive and the substrate. Next, the mechanical theory, which is based on the mechanical interlocking occurring when the adhesive penetrates in the adherend morphology. The third theory is the diffusion theory, based on polymer chain dynamics and the interaction between different polymers.

Recent literature [114] questions the chemical effect of surface modifications on the performance of the adhesive joint, pointing out that performance variations could only be attributed to morphology modifications at the nanoscale. Additive manufacturing offers the possibility to implement integrated surface modifications. This can be done, for example, by mounting an atmospheric plasma torch on the nozzle, or by affecting the surface properties through the printing setup.

The approaches presented in this section were often originally proposed for laminated materials [115, 116], which have certain similarities to additive manufacturing-processed materials, such as a layering effect and an anisotropic behaviour [117]. In the macroscale, adherend modifications can be achieved by including features such as pins or wavy interfaces. In the microscale, additive manufacturing process parameters, such as layer height or nozzle temperatures, can be used to modify surface properties, leading to changes in morphology. The use of mechanical interlocking in additive-manufactured bonded joints is still an open research topic, probably due to the limitations in buildable geometries and the geometrical tolerances achievable with the current additive manufacturing processes.

4 Modelling methods

Modelling of bonded joints is crucial for the implementation of adhesive bonding in modern industrial applications since it allows for predicting joint performance as a function of material properties and design parameters. Thus, it is an indispensable tool for selecting materials and defining the geometry of the joint, which serves to minimise costly

and time-consuming design verification testing and reduce material usage and weight. Joint modelling has traditionally been conducted using analytical models, which, however, are valid only for simple joint geometries and material behaviours. As the geometrical complexity of industrial products increases, so do the geometries of the bonded joints, for which the classical analytical models are not suitable anymore. Consequently, several numerical methods have been developed during the last decades.

4.1 Numerical methods

4.1.1 Linear elasticity

Despite its simplicity, the linear elastic assumption is still employed nowadays for both static strength and fatigue life analyses of bonded joints [118, 119]. Castro Sousa et al. [120] used a linear elastic finite element method to measure an effective stress along the bondline. The same linear elastic assumption has been selected by these authors [121] to obtain the master S–N behaviour of an epoxy-based adhesive.

4.1.2 Hyperelasticity

In hyperelastic models, the adhesive is often assumed to be non-compressible [122, 123], and the strain energy density is used for the hyperelastic analysis [124, 125]. Among the most common hyperelastic models are Mooney–Rivlin [126], neo-Hookean [127], polynomial [124], Yeoh [128], and Ogden [129]. According to Duncan and Dean [130], the first-order hyperelastic model shows more precise results, while other authors, such as Van Lanker et al. [123], suggest using a polynomial model. It has been shown that for small, medium, and large elongations, the neo-Hookean, Mooney–Rivlin, and Ogden models should respectively be used [131]. In more recent years, the effect of void in the hyperelastic response of adhesives has been considered [132, 133]. Moreover, meshless methods have been developed to analyse the stress state in hyperelastic adhesives, especially for materials with a large deformation at failure [134].

4.1.3 Plasticity

Adams et al. [135], Crocombe and Adams [136], Crocombe [137], and Harris and Adams [138] were the first authors to consider the plastic deformation of adhesives. The von Mises criterion is among the most used parameters for assessing plastic flow in bondlines [139]. This criterion has successfully been involved not only in static but also in several fatigue and damage analyses of adhesives [121]. Nevertheless, this criterion does not consider the hydrostatic stresses that can significantly influence the adhesive plastic flow. The Drucker–Prager plasticity model has also been considered [130, 140]. Zgoul and Crocombe [141] compared a strain rate-dependent von Mises model with a strain rate-dependent Drucker–Prager model in shear tests, concluding that the Drucker–Prager model is more accurate.

4.1.4 Fracture in bimaterial interfaces

The generalised stress intensity factor (GSIF) is the most known method for modelling a crack in a bimaterial interface [142, 143]. The stress field in a bimaterial interface is a function of a singularity exponent, a specific distance, and a non-dimensional function:

$$\sigma_{ij} = \sum_{n=1}^{N} H_n r^{-\gamma_n} f_{ij}, \tag{1}$$

where r is the distance from the singular point—(r, θ) are the polar coordinates, with their origin at the singular point; $-\gamma_n$ is the root of the Bogy determinant—see [144, 145]; H_n is the stress intensity factor related to the n-th root determined; and f_{ij} is a non-dimensional function.

The GSIF concept can be used for static and fatigue analyses of adhesive joints. Indeed, it has been recently proposed for strength prediction of SLJs [142, 146].

4.1.5 Damage

The cohesive zone models (CZMs) constitute the most common family of damage models for failure analysis of adhesive joints [147, 148]. The direct method, the reverse method, and the classical models are the main methods used to define the traction–separation law (TSL) in CZM.

Chandra et al. [149] showed that the bilinear TSL is more accurate than the exponential for the materials under consideration. Alfonso [150] stated that the toughness and the stiffness of the adhesive are key parameters in choosing the most appropriate TSL. As a rule, the trapezoidal shape should be used for ductile adhesives, while the bilinear TSL usually presents accurate results for brittle-like materials [151, 152]. May et al. [153] employed the bilinear and trapezoidal shapes for pure mode I loading and pure mode II loading, respectively, while a combination of these two shapes was proposed for mixed-mode loading. Heidari-Rarani and Ghasemi [154] reported a trilinear TSL derived by combining two bilinear TSLs, as shown in Fig. 12.

It should not be overlooked that only the triangular CZM can be used as a built-in model in commercial finite element programmes; for the other TSL shapes, material behaviour should be programmed by the user.

The ductile damage models constitute a second family of damage models, although they have been rarely considered in the failure analysis of adhesive joints. Katsivalis et al. [155] used a combination of a pressure-sensitive Drucker–Prager model with ductile damage to predict the behaviour of bonded glass–steel joints using both a brittle and a ductile adhesive. The model needs to be calibrated using both tension and compression experimental tests. It was shown that their numerical model is insensitive to the mesh size. However, a small change in the strain at break may significantly change the predicted failure load for joints bonded with a brittle adhesive, while the predicted failure load is less sensitive to the elongation at break for ductile adhesive joints.

The extended finite element method (XFEM) is another damage-based numerical approach used to reproduce the mechanical behaviour of adhesive joints. Among its advantages compared to the CZM is its ability to predict the crack path. XFEM is widely used for quasi-static loading conditions, but some authors have also recently used this technique to analyse the fatigue response of adhesive joints [156]. Interestingly, a combination of XFEM and CZM methods has been used in some studies [157, 158]. Despite the advantages of XFEM over CZM, its application for different loading conditions has not yet been sufficiently explored.

4.1.6 Viscoelasticity and viscoplasticity

Due to the viscoelastic nature of adhesives [159], caused by molecular chain movements [160, 161], their mechanical response depends on the loading rate. In addition, due to property degradation caused by specific loading conditions, such as creep and fatigue [161–163], adhesive's viscosity is a function of loading time. Both effects of loading rate and loading time should therefore be considered in modelling the viscoelastic behaviour of adhesives.

Implementing the viscoelastic behaviour into numerical models is achieved using laws described by rate-dependent analytical expressions. The simplest law assumes a linear spring combined with a dashpot [164, 165], while the generalised Maxwell model is among the most recent models [166, 167]. Despite its accuracy, its use is limited due to the large number of constants required to mathematically define the model. Several models using springs and dashpots have been developed for large deformations, chain networks, damage accumulation, cyclic loadings, and strain–softening conditions [168, 169].

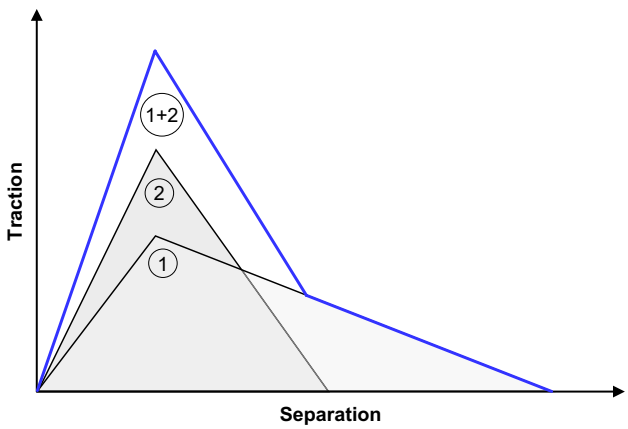

Fig. 12 A typical trilinear CZM made of two bilinear models

It has been shown that a combination of linear and nonlinear springs with a nonlinear dashpot can appropriately consider the effects of strain rate and relaxation [168].

As already mentioned, an interaction of viscosity and loading condition should be considered mainly for joints subjected to fatigue loading or creep. The effect of damage can be considered by using a hyperelastic primary spring arranged parallel to a Maxwell model [170]. Ayoub et al. [171] proposed a visco-hyperelastic model based on the Zener concepts by considering the effect of cyclic loading. In a more recent work, Eslami et al. [172] considered the effects of cyclic loading by developing a phenomenological model where two parallel linear and extended-nonlinear Maxwell elements are used to simulate the adhesive behaviour.

Compared to viscoelasticity, the viscoplastic behaviour of adhesives has received less attention. Perzyna's [173] and G'sell and Jonas's [174] approaches are among the earliest, which have been used further since then [175, 176]. Different combinations of viscoelastic and viscoplastic models have been considered recently [177, 178]. Based on the concepts of Maxwell, Dufour et al. [179] used a coupled viscoelastic–viscoplastic model to simulate the yielding behaviour of adhesives. Likewise, Rocha et al. [180] used a viscoelastic–viscoplastic model to analyse the monotonic and cyclic responses of an epoxy adhesive. In these viscoelastic–viscoplastic approaches, linearity is basically assumed. A nonlinear viscoelastic–viscoplastic response of a film adhesive was considered in a very recent study by Chen and Smith [181]. The finite element results of that work showed that the stress concentration reduces in the presence of viscoplasticity while the strain concentration increases.

4.1.7 Strain rate effects

The ultimate tensile strength of adhesives changes proportionally with the strain rate in a logarithmic scale [182–184]. For a given strain rate, the ultimate tensile strength is lower than the compressive strength [182].

The fracture toughness of adhesives is also strain rate-dependent [185–189]. Nunes et al. [186] showed that even under a constant test speed in a fracture test, the crack-tip strain rate varies with crack size. To consider the effects of strain rate, both rheological models (i.e. using springs and dashpots) and the CZM have been employed. Borges et al. [185] proposed a strain rate-dependent CZM, adjusted for mode I loading conditions, where the TSL is a function of the strain rate that each material point experiences at each loading increment.

CZM concepts were also employed by Machado et al. [190] for the rate-dependent analysis of adhesives. The linear elastic assumption has also been considered in some studies to numerically study the effect of strain rate [191]. The Johnson–Cook and Cowper–Symonds models [192] are the two strain rate-dependent models typically used in numerical simulations. Among them, the second model can more accurately simulate the interfacial stresses [193, 194] and has recently been used by several authors [195, 196].

4.1.8 Water uptake

Extensive studies have been conducted to experimentally analyse the deterioration effects of humidity on the mechanical response of adhesives [79, 197, 198]. A heat transfer analogy is usually used to simulate the water uptake behaviour in adhesive joints: the nodal temperature corresponds to the level of water in a particular material point, while the thermal conductivity corresponds to the water diffusion coefficient. The boundary condition should be defined as the saturation level obtained experimentally.

Not only the water uptake process but also the drying process needs to be simulated [197, 199]. Simulating both processes is essential for bonded joints, which are subjected to cyclic ageing loading in practice that includes water absorption and desorption cycles. Numerical modelling in cyclic ageing is similar to that for a single-cycle water uptake process. Nevertheless, different diffusion coefficients should be defined for each cycle, while also the boundary conditions depend on the ageing cycle [197]. Very recently, the static strength [197], fracture energy [200], and fatigue life [201] of bonded joints have been investigated under cyclic ageing conditions. It was shown that using a single-cycle ageing result may overestimate the strength and lifetime of bonded joints exposed to cyclic moisture.

4.2 Failure and life-prediction models

4.2.1 Fracture mechanics models

Crack initiation and its propagation path in bonded joints have been studied by several authors [202, 203]. The so-called maximum tangential stress (MTS), strain energy density (SED), and maximum tangential strain energy density (MTSED)

approaches are well-known in the fracture mechanics-based analysis of adhesive joints [143, 204]. According to the MTS method, tangential stress is a key stress component that governs the failure in bonded joints. Based on the SED method, crack propagation occurs along a direction where the SED reaches a critical value at a critical distance. Lastly, the MTSED method combines the concepts of the previous two methods.

Akhavan-Safar et al. [143] employed these approaches to predict the static failure load of adhesive joints. The crack-kinking angle, critical distance, and critical tangential SED are the three parameters that the MTSED model uses for failure prediction in cracked bonded joints. The results showed that the crack-kinking angle is more precisely predicted by SED for mode I-dominated conditions, while MTS is a more appropriate choice when mode II fracture is predominant [143]. The effect of T-stress has also been considered in some studies [202, 205], and it was shown that a more stable crack propagation is assured when the T-stress has a negative value [206].

Finite fracture mechanics is another fracture mechanics-based approach that has recently attracted significant research attention [207]. Several research groups have numerically implemented this approach to investigate different types of adhesive joints [208–210]. We should not overlook that the effect of nonlinearities of the adherends or the joint must be negligible using this approach [211, 212].

GSIF is another technique used to evaluate the stress intensity factor at bimaterial interfaces, including the interface between adhesive and adherend, as shown in Fig. 13 [142]. Although Groth [213] considered the critical GSIF as a material constant, this parameter also depends on the geometry of the joint [142, 214]. Akhavan-Safar et al. [142] showed that the overlap length significantly influences the critical value of the GSIF, H_c. The authors also showed that using a thinner bondline pronounces the effect of adherend thickness on H_c. Ayatollahi et al. [214] studied the effect of the bimaterial notch angle on the GSIF. GSIF is more accurate for the failure analysis of joints made of brittle or semi-brittle materials. Interestingly, Rastegar et al. [146] recently combined the GSIF method with analytical models to predict the static strength of adhesively bonded SLJs.

A major drawback of the GSIF-based methods is their dependency on the mesh size. To overcome this issue, Zhang et al. [215] suggested using a so-called ratio method, where the ratio of GSIFs for two SLJs with different overlap lengths is assumed constant. The method was later extended to SLJs with different adherend thicknesses [146].

4.2.2 Damage mechanics models

Continuum damage mechanics and CZM are the two most widely used damage mechanics models, using fracture energy as a key failure parameter that should be obtained experimentally [143, 185, 188, 189, 203, 216]. Continuum damage mechanics is based on stiffness degradation due to damage evolution [217, 218]. For the damaged area, different behaviours can be assumed, including the linear elastic, plastic (e.g. Drucker–Prager model), and nonlinear behaviours, as well as different damage evolution shapes, such as linear [219]. Zhang et al. [220] and Kim and Hong [221] showed that the effect of mode mixity on the damage parameter should also be considered.

CZM is more commonly considered than continuum damage mechanics for the failure analysis of adhesive materials. A comparison between these two methods showed that CZM is generally more accurate. Continuum damage mechanics is, however, capable of predicting the crack path, while in CZM, the crack path should be predefined [222].

Different classical CZM shapes have been considered to predict the mechanical response of adhesives, while customised shapes are also a usual choice. Some authors argue that the accuracy of the bilinear CZM shape is sufficient for the

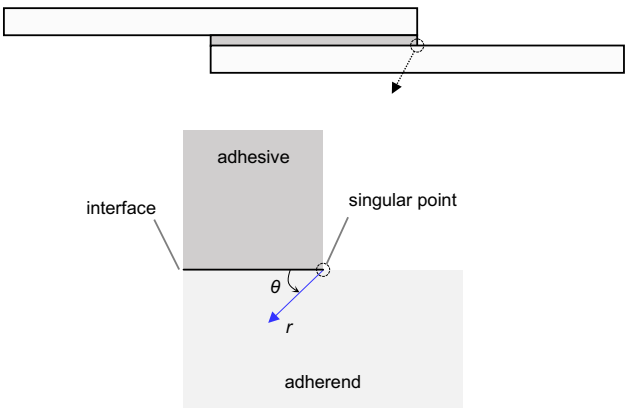

Fig. 13 Singular points and bimaterial interface in a SLJ

purpose of predicting the joint's strength [149, 223]. Other studies have shown that the trapezoidal CZM shape provides more accurate results than the bilinear shape for ductile adhesives [152, 224]. A combined bilinear and trapezoidal CZM shape was considered by May et al. [153], and their results showed that this shape is loading mode dependent. Specifically, for pure mode I and pure mode II conditions, a bilinear and a trapezoidal shape should respectively be used. For mixed-mode I/II conditions, the authors introduced a pseudo-plasticity parameter to define the CZM shape. To consider different failure mechanisms, a trilinear CZM shape was recently proposed [154]. Lastly, to choose the most appropriate CZM shape, a ratio between the toughness and the stiffness has been proposed in Ref. [150].

4.2.3 Fatigue models

Models developed for the fatigue life analysis of adhesive joints are generally divided into three groups: S–N models, which mainly consider the damage initiation phase; fatigue crack growth models, which consider the crack propagation phase; and cohesive zone models, where both the initiation and propagation phases are considered.

4.2.3.1 S–N models In the S–N approach, the main steps are two: first, to correctly define a fatigue parameter; and second, to define a material point (critical distance) where this parameter should be measured. Variations in fatigue parameters and the different definitions that have been proposed for the critical distance have resulted in different S–N models. Moreover, environmental conditions affect fatigue performance and should therefore be considered by the fatigue models [225–228].

Jen [229] correlated the von Mises stress (in cohesive failure mode) and peel stress (in adhesive failure mode) with fatigue life in scarf joints. By considering the effect of mode mixity, Castro Sousa et al. [120, 121] proposed an equivalent fatigue stress parameter considering von Mises and hydrostatic stresses. The proposed model can correlate well with the fatigue life of the tested joints. The same concept was used for the lifetime assessment of a real bonded component used in agricultural vehicles [230]. The von Mises equivalent stress and Drucker–Prager criterion were compared by Beber et al. [231], and it was found that the von Mises-based model is more accurate for scarf joints, while the Drucker–Prager method is suggested for SLJs.

Among the recent S–N-based methods used for fatigue life analysis of adhesive joints are the critical distance/plane approaches [232]. Smith–Watson–Topper is among the most used methods that was suggested by Shahani and Pourhosseini [233] and Pereira et al. [234], while the Crossland model [235] appeared not accurate enough for the joints tested by the authors. Critical distance/plane methods were also recently considered for epoxy bonded joints [236].

The GSIF concept has also been used for fatigue initiation analysis of adhesive joints [237, 238]. GSIF can be used to estimate the fatigue life of adhesives, where there is a small plastic zone at the singular point. Using GSIF and a 3-D fatigue initiation surface, Lefebvre et al. [238] analysed the fatigue life of bonded assemblies.

4.2.3.2 Fatigue crack growth models The damage tolerance philosophy is used to extend the service life of structural components and reduce structural weight. Based on this philosophy, the life spent on fatigue crack growth should be considered [239, 240]. However, several parameters affect the fatigue response of adhesive joints, rendering it challenging to develop a general model [241].

By modifying the Paris-law relationship, researchers have attempted to consider the effects of influencing parameters. Rocha et al. [242] investigated different Paris-law relations for joints subjected to mode I fatigue loading conditions. The authors found that considering R-ratio effects and using the maximum energy release rate corresponding to each loading cycle, the Paris-law curve can be collapsed into a single master curve. The effect of loading conditions was also investigated by Chen et al. [243] by including a mixed-mode parameter in the Paris-law relation. Not only the variety in loading and environmental conditions [201, 227], but also the difference in joint geometry—especially the adhesive thickness—can change the fatigue crack growth rate [244, 245].

4.2.3.3 Cohesive zone models (CZMs) As a widely used damage model, CZM can predict both the initiation and propagation phases [147]. Two types of CZMs have been used for the fatigue analysis of adhesives: cycle-by-cycle models and failure envelope models.

The first type is more used for the low-cycle fatigue regime while the second one is more considered for high-cycle fatigue conditions. In the failure envelope strategy, the rate of damage evolution per loading cycle can be obtained either through linking the damage mechanics and fracture mechanics together—*linking damage mechanics and fracture mechanics* method [246]—or through fitting, where the damage function can be stress-based [247] or strain-based [248].

The *linking damage mechanics and fracture mechanics* method is more automated and has been used by several authors recently [249, 250] while the fitting method is easier to implement in finite element programmes.

Considering the static damage induced by fatigue degradation, a CZM-based fatigue model was recently proposed by Ebadi-Rajoli et al. [251], where a normalised strain energy in the context of Paris law was used to simulate crack propagation. This model is schematically shown in Fig. 14.

Using CZM, not only the constant-amplitude fatigue loading but also the lifetime of joints subjected to variable-amplitude fatigue loading conditions can be predicted [252]. A detailed review and discussion on the application of CZM for the fatigue life analysis of adhesive joints are available in Ref. [161].

4.2.4 Creep models

The two major classes of models to predict creep behaviour are the rheological models and power-law or empirical models.

Maxwell and Kelvin models are the simplest rheological models. However, Maxwell's model does not consider the relaxation phenomenon, while Kelvin's model does not show satisfactory results for polymers [253]. Burger's model combines these two models [254, 255]. Majda and Skrodzewicz [256], Houhou et al. [257], and Ashofteh and Khoramishad [258] have considered Burger's model to investigate the creep behaviour of adhesives. More complex creep models have also been developed by adding more elements and assuming a nonlinear behaviour for each element to consider different phenomena, such as relaxation [259]. A generalised Maxwell model was used by Hamed and Chang [260]. Likewise, Choi and Reda Taha [261] successfully employed an extended Maxwell model.

Power-law and empirical models are the second, widely used family of models for investigating the creep behaviour of adhesive joints [262, 263]. By adding nanoparticles in Ref. [264], the creep performance was enhanced, and some empirical models were developed to include the effects of nano-additives in creep life analysis [263]. According to the literature, viscoplasticity must be considered when the creep stress is high.

Numerical modelling of creep behaviour has been widely used, typically employing CZM [163, 265]. For example, Carneiro Neto et al. [163] developed a CZM for damage analysis of joints subjected to creep. Xu et al. [266] employed continuum damage mechanics to simulate the creep of adhesives, also considering the effect of temperature on viscosity. The same effect was considered by Marques et al. [267], who proposed a master curve to predict the creep life of aluminium-to-glass adhesive joints.

4.3 Multiphysics modelling

Multiphysics modelling is increasingly used to simulate phenomena or processes that combine different analysis classes, such as structural mechanics, fluid dynamics, thermal flow, mass diffusion, chemical reactions, and particle tracing [58, 268]. Multiphysics models can lead to a complete characterisation and optimisation of behaviours or processes, but they require as inputs several different material properties [58]. Multiphysics modelling of problems that include adhesive bonding is an emerging topic. Zhang et al. [269] studied piezoelectric sensors used in acoustic emission. A numerical simulation was conducted using a multiphysics software, considering the source function, steel plate, and piezoelectric sensor, and detailing the adhesive layer, wear plate, piezoelectric ceramic, and backing

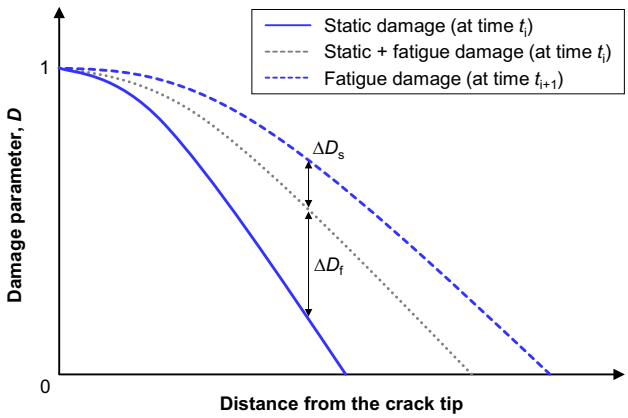

Fig. 14 Effect of fatigue damage on static damage

material. This study was based on previous research that combined the structural wave propagation and sensor model using multiphysics [270]. da Silva et al. [58] aimed to create a functionally graded adhesive through the introduction of iron microparticles dispersed in a polyurethane adhesive. The distribution of the particles should create a gradient, with a higher concentration in the middle of the overlap and lower at the ends. The COMSOL Multiphysics® software was used to numerically simulate the particle dispersion inside the adhesive, under the effect of magnet arrangements placed outside the adhesive layer. Both the magnetic properties of the particles and the interaction with the viscous medium in which they move must be considered. The numerical simulation was validated against experimental results in an SLJ.

Katsivalis et al. [270] used the Multiphysics capability of Abaqus software to simulate the moisture ingress into a glass/adhesive interface, followed by the coupled mechanical analysis using diffusion effects and CZM for damage studies. The numerical model was calibrated using a double cantilever beam specimen, and then, it correctly simulated the exposure time for partial and total joint degradation of a large DLJ, which has a different geometry from the double cantilever beam specimen.

5 Concluding remarks

Adhesive bonding is a constantly growing research field due to the increasing interest it receives from the industry. The research activity in this field can be divided into several sub-disciplines, such as adhesive materials, design and manufacturing concepts, and modelling approaches.

Regarding adhesive materials, it was seen that in the group of structural adhesives, the second- and third-generation acrylics allow a fast application and curing and can be used to change the adhesive's properties by altering the ratio between the two components. Toughened epoxies have been presented as an alternative to the classical adhesive types, increasing the fracture toughness of the material and making it suitable for, for instance, automotive and aeronautical applications. Two-component polyurethanes have also been developed as an alternative to the conventional one-component materials, being used in structural applications, with high ductility and fracture toughness. In the group of non-structural adhesives, PSAs have been adopted in more applications due to the simplicity and cleanness of the application process, as well as the availability of PSAs manufactured from different adhesive families to have the appropriate properties for each application. A clear trend in using bio-based adhesives has also been observed, promoted by the need to decrease the environmental footprint of these materials, mainly for non-structural applications.

As known, adhesive joints commonly operate in shear, and their behaviour is often evaluated using SLJs that show a stress concentration at the overlap ends. Different design approaches can be employed to decrease this stress concentration, taking advantage of the use of functionally graded adhesives or adherends. In addition, adhesive bonding can be used in combination with other joining methods, such as bolting, riveting, clinching, and welding, to improve joint strength and durability.

From a modelling perspective, several alternative methods have been developed to account for the effects of various parameters that can significantly affect the mechanical behaviour of bonded structures. Although most analytical models can predict the stress state for simple joint geometries, numerical techniques are preferred nowadays for the failure analysis and lifetime prediction of adhesive joints. Models based on continuum mechanics and fracture mechanics have been extensively studied for the durability analysis of different materials. Nevertheless, due to their certain limitations, damage mechanics models, especially the CZM approach, are usually considered for the fracture analysis of adhesives. The capability of the CZM to simulate long-term loads, such as fatigue or creep, has also been reported in the literature.

Acknowledgements This research was funded by the project No. PTDC/EME-EME/6442/2020 'A smart and eco-friendly adhesively bonded structure for the next generation mobility platforms' and the individual Grant No. 2020.04017.CEECIND, funded by national funds through the Portuguese Foundation for Science and Technology (FCT).

Author contributions CSPB, AA-S, and PT wrote the initial and final manuscripts. CSPB and AA-S prepared the initial figures. PT prepared the final figures. RJCC, EASM, and LFMdS reviewed the initial and final manuscripts. All authors accepted the initial and final manuscripts.

Declarations

Competing interests The authors declare no competing interests.

Data availability Data sharing is not applicable to this article as no new data were created or analyzed in this study.

References

1. da Silva LFM, Öchsner A, Adams RD, editors. Handbook of adhesion technology. 2nd ed. Springer Cham; 2018. https://doi.org/10.1007/978-3-319-55411-2.
2. Fay PA. A history of adhesive bonding. In: Adams RD, editor. Adhesive bonding. Woodhead Publishing; 2021. p. 3–40. https://doi.org/10.1016/B978-0-12-819954-1.00017-4.
3. Skeist I, Miron J. History of adhesives. J Macromol Sci Part A Chem. 1981;15(6):1151–63. https://doi.org/10.1080/00222338108066458.
4. Aronovich DA, Boinovich LB. Structural acrylic adhesives: a critical review. In: Mittal KL, editor. Progress in adhesion and adhesives. Scrivener Publishing LLC; 2021. p. 651–708. https://doi.org/10.1002/9781119846703.ch15.
5. Sekiguchi Y, Nakanouchi M, Haraga K, Takasaki I, Sato C. Experimental investigation on strength of stepwise tailored single lap adhesive joint using second-generation acrylic adhesive via shear and low-cycle shear tests. Int J Adhes Adhes. 2019;95:102438. https://doi.org/10.1016/j.ijadhadh.2019.102438.
6. Nakanouchi M, Sato C, Sekiguchi Y, Haraga K, Uno H. Development of application method for fabricating functionally graded adhesive joints by two-component acrylic adhesives with different elastic moduli. J Adhes. 2019;95(5–7):529–42. https://doi.org/10.1080/00218464.2019.1583562.
7. Iwata T, Hayashibara H. Durability and flammability evaluation of SGA structural adhesive joints consisting of a thick adhesive layer for shipbuilding. J Adhes. 2019;95(5–7):614–31. https://doi.org/10.1080/00218464.2019.1581067.
8. Hayashi A, Sekiguchi Y, Sato C. AFM observation of sea-island structure formed by second generation acrylic adhesive. J Adhes. 2021;97(2):155–71. https://doi.org/10.1080/00218464.2019.1649148.
9. Kamiyama K, Mikuni M, Matsumoto T. Fracture propagation analysis on two component type acrylic adhesive joints. Int J Adhes Adhes. 2018;83:76–86. https://doi.org/10.1016/j.ijadhadh.2018.02.019.
10. May C. Epoxy resins: chemistry and technology. 2nd ed. Routledge; 2018.
11. Kausar A. Rubber toughened epoxy-based nanocomposite: a promising pathway toward advanced materials. J Macromol Sci Part A. 2020;57(7):499–511. https://doi.org/10.1080/10601325.2020.1730190.
12. Garg AC, Mai Y-W. Failure mechanisms in toughened epoxy resins—a review. Compos Sci Technol. 1988;31(3):179–223. https://doi.org/10.1016/0266-3538(88)90009-7.
13. Bagheri R, Marouf BT, Pearson RA. Rubber-toughened epoxies: a critical review. J Macromol Sci Part C Polymer Rev. 2009;49(3):201–25. https://doi.org/10.1080/15583720903048227.
14. Mousavi SR, Estaji S, Raouf Javidi M, Paydayesh A, Khonakdar HA, Arjmand M, et al. Toughening of epoxy resin systems using core–shell rubber particles: a literature review. J Mater Sci. 2021;56:18345–67. https://doi.org/10.1007/s10853-021-06329-8.
15. Szycher M, editor. Szycher's handbook of polyurethanes. 2nd ed. CRC Press; 2012. https://doi.org/10.1201/b12343.
16. Zimmer B, Nies C, Schmitt C, Possart W. Chemistry, polymer dynamics and mechanical properties of a two-part polyurethane elastomer during and after crosslinking. Part I: dry conditions. Polymer. 2017;115:77–95. https://doi.org/10.1016/j.polymer.2017.03.020.
17. Brains P. Polyurethanes technology. Wiley; 1969.
18. Banea MD, da Silva LFM, Campilho RDSG. The effect of adhesive thickness on the mechanical behavior of a structural polyurethane adhesive. J Adhes. 2015;91(5):331–46. https://doi.org/10.1080/00218464.2014.903802.
19. Zimmer B, Nies C, Schmitt C, Paulo C, Possart W. Chemistry, polymer dynamics and mechanical properties of a two-part polyurethane elastomer during and after crosslinking. Part II: moist conditions. Polymer. 2018;149:238–52. https://doi.org/10.1016/j.polymer.2018.06.070.
20. Huacuja-Sánchez JE, Müller K, Possart W. Water diffusion in a crosslinked polyether-based polyurethane adhesive. Int J Adhes Adhes. 2016;66:167–75. https://doi.org/10.1016/j.ijadhadh.2016.01.005.
21. Ogawa Y, Naito K, Harada K, Oguma H. Evaluation of crack growth behaviors under Mode I static loading for two-part polyurethane adhesives. Int J Adhes Adhes. 2022;117(A):103172. https://doi.org/10.1016/j.ijadhadh.2022.103172.
22. Landrock AH. Adhesives technology handbook. Noyes Publications; 1985.
23. Mapari S, Mestry S, Mhaske ST. Developments in pressure-sensitive adhesives: a review. Polym Bull. 2021;78:4075–108. https://doi.org/10.1007/s00289-020-03305-1.
24. Deshpande A, Song Z, Vaidya SA. Creep model for pressure sensitive adhesives under shear load. In: Proceedings of the 2020 Asia-Pacific International Symposium on Advanced Reliability and Maintenance Modeling, Vancouver, BC, Canada; 2020. p. 1–5.
25. Baek S-S, Hwang S-H. Eco-friendly UV-curable pressure sensitive adhesives containing acryloyl derivatives of monosaccharides and their adhesive performances. Int J Adhes Adhes. 2016;70:110–6. https://doi.org/10.1016/j.ijadhadh.2016.06.002.
26. Baek S-S, Hwang S-H. Preparation of biomass-based transparent pressure sensitive adhesives for optically clear adhesive and their adhesion performance. Eur Polymer J. 2017;92:97–104. https://doi.org/10.1016/j.eurpolymj.2017.04.039.

27. Shibakami M, Sohma M. Thermal, crystalline, and pressure-sensitive adhesive properties of paramylon monoesters derived from an euglenoid polysaccharide. Carbohyd Polym. 2018;200:239–47. https://doi.org/10.1016/j.carbpol.2018.08.005.
28. Fuensanta M, Martin-Martínez JM. Thermoplastic polyurethane pressure sensitive adhesives made with mixtures of polypropylene glycols of different molecular weights. Int J Adhes Adhes. 2019;88:81–90. https://doi.org/10.1016/j.ijadhadh.2018.11.002.
29. Lin SB. New silicone pressure-sensitive adhesive technology. Int J Adhes Adhes. 1994;14(3):185–91. https://doi.org/10.1016/0143-7496(94)90029-9.
30. Montméat P, Enot T, De Marco DM, Pellat M, Fournel F. Study of a silicon/glass bonded structure with a UV-curable adhesive for temporary bonding applications. Microelectron Eng. 2017;173:13–21. https://doi.org/10.1016/j.mee.2017.03.008.
31. Khan I, Poh BT. Natural rubber-based pressure-sensitive adhesives: a review. J Polym Environ. 2011;19:793–811. https://doi.org/10.1007/s10924-011-0299-z.
32. Chung S-W, Kwak JB. A novel evaluation of shock absorption and adhesive strength under shear impact loading. J Adhes. 2021;97(16):1578–94. https://doi.org/10.1080/00218464.2020.1804375.
33. Son H, Erk KA, Davis CS. Substrate temperature effects on the peel behavior of temporary pavement marking tapes. J Adhes. 2023;99(2):153–65. https://doi.org/10.1080/00218464.2021.2008369.
34. Hogger EM, van Herwijnen HWG, Moser J, Kantner W, Konnerth J. Systematic assessment of wheat extenders in condensation resins for plywood production: part I-physico-chemical adhesive properties. J Adhes. 2021;97(15):1404–22. https://doi.org/10.1080/00218464.2020.1776123.
35. Arias A, González-Rodríguez S, Vetroni Barros M, Salvador R, de Francisco AC, Moro Piekarski C, et al. Recent developments in bio-based adhesives from renewable natural resources. J Clean Prod. 2021;314:127892. https://doi.org/10.1016/j.jclepro.2021.127892.
36. Dongre P, Driscoll M, Amidon T, Bujanovic B. Lignin-furfural based adhesives. Energies. 2015;8(8):7897–914. https://doi.org/10.3390/en8087897.
37. Chen X, Xi X, Pizzi A, Fredon E, Du G, Gerardin C, et al. Oxidized demethylated lignin as a bio-based adhesive for wood bonding. J Adhes. 2021;97(9):873–90. https://doi.org/10.1080/00218464.2019.1710830.
38. Lubis MAR, Park B-D. Enhancing the performance of low molar ratio urea–formaldehyde resin adhesives via in-situ modification with intercalated nanoclay. J Adhes. 2021;97(14):1271–90. https://doi.org/10.1080/00218464.2020.1753515.
39. Tejado A, Peña C, Labidi J, Echeverria JM, Mondragon I. Physico-chemical characterization of lignins from different sources for use in phenol-formaldehyde resin synthesis. Bioresour Technol. 2007;98(8):1655–63. https://doi.org/10.1016/j.biortech.2006.05.042.
40. Khosravi S, Khabbaz F, Nordqvist P, Johansson M. Protein-based adhesives for particleboards. Ind Crops Prod. 2010;32(3):275–83. https://doi.org/10.1016/j.indcrop.2010.05.001.
41. Pizzi A, Mittal KL, editors. Wood adhesives. 1st ed. CRC Press; 2011.
42. Pizzi A. Recent developments in eco-efficient bio-based adhesives for wood bonding: opportunities and issues. J Adhes Sci Technol. 2006;20(8):829–46. https://doi.org/10.1163/156856106777638635.
43. Zhong Z, Sun XS, Wang D, Ratto JA. Wet strength and water resistance of modified soy protein adhesives and effects of drying treatment. J Polym Environ. 2003;11:137–44. https://doi.org/10.1023/A:1026048213787.
44. Borges CSP, Jalali S, Tsokanas P, Marques EAS, Carbas RJC, da Silva LFM. Sustainable development approaches through wooden adhesive joints design. Polymers. 2023;15(1):89. https://doi.org/10.3390/polym15010089.
45. Raphael C. Variable-adhesive bonded joints (Stresses in ordinary lap joint compared to variable adhesive joint). In: Structural adhesives bonding, Symposium, Stevens Inst. of Tech, Hoboken, NJ. 1966.
46. Hart-Smith LJ. Adhesive-bonded double-lap joints. NASA CR-1122 36. 1973.
47. Pires I, Quintino L, Durodola JF, Beevers A. Performance of bi-adhesive bonded aluminium lap joints. Int J Adhes Adhes. 2003;23(3):215–23. https://doi.org/10.1016/S0143-7496(03)00024-1.
48. Fitton MD, Broughton JG. Variable modulus adhesives: an approach to optimised joint performance. Int J Adhes Adhes. 2005;25(4):329–36. https://doi.org/10.1016/j.ijadhadh.2004.08.002.
49. da Silva LFM, Lopes MJCQ. Joint strength optimization by the mixed-adhesive technique. Int J Adhes Adhes. 2009;29(5):509–14. https://doi.org/10.1016/j.ijadhadh.2008.09.009.
50. Temiz Ş. Application of bi-adhesive in double-strap joints subjected to bending moment. J Adhes Sci Technol. 2006;20(14):1547–60. https://doi.org/10.1163/156856106778884262.
51. das Neves PJC, da Silva LFM, Adams RD. Analysis of mixed adhesive bonded joints Part I: theoretical formulation. J Adhes Sci Technol. 2009;23(1):1–34. https://doi.org/10.1163/156856108X336026.
52. Marques EAS, da Silva LFM. Joint strength optimization of adhesively bonded patches. J Adhes. 2008;84(11):915–34. https://doi.org/10.1080/00218460802505275.
53. da Silva LFM, Adams RD. Adhesive joints at high and low temperatures using similar and dissimilar adherends and dual adhesives. Int J Adhes Adhes. 2007;27(3):216–26. https://doi.org/10.1016/j.ijadhadh.2006.04.002.
54. Sancaktar E, Kumar S. Selective use of rubber toughening to optimize lap-joint strength. J Adhes Sci Technol. 2000;14(10):1265–96. https://doi.org/10.1163/156856100742195.
55. Bagheri R, Pearson RA. Role of particle cavitation in rubber-toughened epoxies: II. Inter-particle distance. Polymer. 2000;41(1):269–76. https://doi.org/10.1016/S0032-3861(99)00126-3.
56. Stapleton SE, Waas AM, Arnold SM. Functionally graded adhesives for composite joints. Int J Adhes Adhes. 2012;35:36–49. https://doi.org/10.1016/j.ijadhadh.2011.11.010.
57. Silva CI, Barbosa AQ, Marques JB, Carbas RJC, Marques EAS, Abenojar J, et al. Mechanical characterisation of graded single lap joints using magnetised cork microparticles. In: da Silva L, Martins P, El-Zein M, editors. Advanced joining processes. Advanced structured materials, vol. 125. Springer; 2020. p. 153–74. https://doi.org/10.1007/978-981-15-2957-3_11.
58. da Silva CI, Cunha MRO, Barbosa AQ, Carbas RJC, Marques EAS, da Silva LFM. Functionally graded adhesive joints using magnetic microparticles with a polyurethane adhesive. J Adv Join Proc. 2021;3:100048. https://doi.org/10.1016/j.jajp.2021.100048.
59. Kumar S. Analysis of tubular adhesive joints with a functionally modulus graded bondline subjected to axial loads. Int J Adhes Adhes. 2009;29(8):785–95. https://doi.org/10.1016/j.ijadhadh.2009.06.006.

60. Kumar S, Scanlan JP. On axisymmetric adhesive joints with graded interface stiffness. Int J Adhes Adhes. 2013;41:57–72. https://doi.org/10.1016/j.ijadhadh.2012.09.001.
61. Carbas RJC, da Silva LFM, Marques EAS, Lopes AM. Effect of post-cure on the glass transition temperature and mechanical properties of epoxy adhesives. J Adhes Sci Technol. 2013;27(23):2542–57. https://doi.org/10.1080/01694243.2013.790294.
62. Carbas RJC, da Silva LFM, Critchlow GW. Adhesively bonded functionally graded joints by induction heating. Int J Adhes Adhes. 2014;48:110–8. https://doi.org/10.1016/j.ijadhadh.2013.09.045.
63. Carbas R, Silva L, Critchlow G. Effect of post-cure on adhesively bonded functionally graded joints by induction heating. Proc Inst Mech Eng L J Mater Des Appl. 2015;229(5):419–30. https://doi.org/10.1177/1464420714523579.
64. Carbas RJC, Viana GMSO, da Silva LFM, Critchlow GW. Functionally graded adhesive patch repairs of wood beams in civil applications. J Compos Constr. 2015;19(2):04014038. https://doi.org/10.1061/(ASCE)CC.1943-5614.0000500.
65. Kawasaki S, Nakajima G, Haraga K, Sato C. Functionally graded adhesive joints bonded by honeymoon adhesion using two types of second generation acrylic adhesives of two components. J Adhes. 2016;92(7–9):517–34. https://doi.org/10.1080/00218464.2015.1113525.
66. dos Reis MQ, Marques EAS, Carbas RJC, da Silva LFM. Functionally graded adherends in adhesive joints: an overview. J Adv Join Proc. 2020;2:100033. https://doi.org/10.1016/j.jajp.2020.100033.
67. Ganesh VK, Choo TS. Modulus graded composite adherends for single-lap bonded joints. J Compos Mater. 2002;36(14):1757–67. https://doi.org/10.1177/0021998302036014172.
68. Boss JN, Ganesh VK, Lim CT. Modulus grading versus geometrical grading of composite adherends in single-lap bonded joints. Compos Struct. 2003;62(1):113–21. https://doi.org/10.1016/S0263-8223(03)00097-7.
69. Apalak MK, Gunes R. Investigation of elastic stresses in an adhesively bonded single lap joint with functionally graded adherends in tension. Compos Struct. 2005;70(4):444–67. https://doi.org/10.1016/j.compstruct.2004.09.004.
70. Apalak MK, Gunes R. Elastic flexural behaviour of an adhesively bonded single lap joint with functionally graded adherends. Mater Des. 2007;28(5):1597–617. https://doi.org/10.1016/j.matdes.2006.02.013.
71. Melograna JD, Grenestedt JL. Improving joints between composites and steel using perforations. Compos A Appl Sci Manuf. 2002;33(9):1253–61. https://doi.org/10.1016/S1359-835X(02)00050-7.
72. Kumar S, de Tejada Alvarez A. Modeling and experimental evaluation of geometrically graded multi-material single-lap joints. In: 56th AIAA/ASCE/AHS/ASC Structures, Structural Dynamics, and Materials Conference. 2015.
73. Chen P, Guo W, Zhao Y, Li E, Yang Y, Liu H. Numerical analysis of the strength and interfacial properties of adhesive joints with graded adherends. Int J Adhes Adhes. 2019;90:88–96. https://doi.org/10.1016/j.ijadhadh.2019.02.003.
74. da Silva LFM, Pirondi A, Öchsne A, editors. Hybrid adhesive joints. Berlin: Springer; 2011. https://doi.org/10.1007/978-3-642-16623-5.
75. Caccese V, Kabche J-P, Berube KA. Analysis of a hybrid composite/metal bolted connection subjected to flexural loading. Compos Struct. 2007;81(3):450–62. https://doi.org/10.1016/j.compstruct.2006.09.009.
76. Matsuzaki R, Shibata M, Todoroki A. Improving performance of GFRP/aluminum single lap joints using bolted/co-cured hybrid method. Compos A Appl Sci Manuf. 2008;39(2):154–63. https://doi.org/10.1016/j.compositesa.2007.11.009.
77. Barut A, Madenci E. Analysis of bolted–bonded composite single-lap joints under combined in-plane and transverse loading. Compos Struct. 2009;88(4):579–94. https://doi.org/10.1016/j.compstruct.2008.06.003.
78. Boretzki J, Albiez M. Static strength and load bearing behaviour of hybrid bonded bolted joints: experimental and numerical investigations. J Adhes. 2023;99(4):606–31. https://doi.org/10.1080/00218464.2022.2033619.
79. Delzendehrooy F, Akhavan-Safar A, Barbosa AQ, Carbas RJC, Marques EAS, da Silva LFM. Investigation of the mechanical performance of hybrid bolted-bonded joints subjected to different ageing conditions: effect of geometrical parameters and bolt size. J Adv Join Proc. 2022;5:100098. https://doi.org/10.1016/j.jajp.2022.100098.
80. Pirondi A, Moroni F. Clinch-bonded and rivet-bonded hybrid joints: application of damage models for simulation of forming and failure. J Adhes Sci Technol. 2009;23(10–11):1547–74. https://doi.org/10.1163/156856109X433063.
81. Sadowski T, Kneć M, Golewski P. Experimental investigations and numerical modelling of steel adhesive joints reinforced by rivets. Int J Adhes Adhes. 2010;30(5):338–46. https://doi.org/10.1016/j.ijadhadh.2009.11.004.
82. Sadowski T, Golewski P, Zarzeka-Raczkowska E. Damage and failure processes of hybrid joints: adhesive bonded aluminium plates reinforced by rivets. Comput Mater Sci. 2011;50(4):1256–62. https://doi.org/10.1016/j.commatsci.2010.06.022.
83. Sadowski T, Zarzeka-Raczkowska E. Hybrid adhesive bonded and riveted joints—influence of rivet geometrical layout on strength of joints. Arch Metall Mater. 2012;57:1128–35. https://doi.org/10.2478/V10172-012-0126-0.
84. Solmaz MY, Topkaya T. Progressive failure analysis in adhesively, riveted, and hybrid bonded double-lap joints. J Adhes. 2013;89(11):822–36. https://doi.org/10.1080/00218464.2013.765800.
85. Liu Y, Zhang L, Liu W, Wang PC. Single-sided piercing riveting for adhesive bonding in vehicle body assembly. J Manuf Syst. 2013;32(3):498–504. https://doi.org/10.1016/j.jmsy.2013.04.005.
86. Fiore V, Alagna F, Galtieri G, Borsellino C, Di Bella G, Valenza A. Effect of curing time on the performances of hybrid/mixed joints. Compos B Eng. 2013;45(1):911–8. https://doi.org/10.1016/j.compositesb.2012.05.016.
87. Jiang H, Liao Y, Jing L, Gao S, Li G, Cui J. Mechanical properties and corrosion behavior of galvanized steel/Al dissimilar joints. Arch Civil Mech Eng. 2021;21:168. https://doi.org/10.1007/s43452-021-00320-5.
88. Ibrahim AH, Cronin DS. Mechanical testing of adhesive, self-piercing rivet, and hybrid jointed aluminum under tension loading. Int J Adhes Adhes. 2022;113:103066. https://doi.org/10.1016/j.ijadhadh.2021.103066.
89. Balawender T, Sadowski T, Golewski P. Numerical analysis and experiments of the clinch-bonded joint subjected to uniaxial tension. Comput Mater Sci. 2012;64:270–2. https://doi.org/10.1016/j.commatsci.2012.05.014.
90. Moroni F. Fatigue behaviour of hybrid clinch-bonded and self-piercing rivet bonded joints. J Adhes. 2019;95(5–7):577–94. https://doi.org/10.1080/00218464.2018.1552586.
91. Zhuang W, Shi H, Li M. Curing effects on forming and mechanical performance of clinch-adhesive joints of dissimilar materials between AA5754 Aluminum Alloy and Q235 steel. J Adhes. 2023;99(1):1–33. https://doi.org/10.1080/00218464.2021.1996238.

92. Moroni F, Pirondi A, Kleiner F. Experimental analysis and comparison of the strength of simple and hybrid structural joints. Int J Adhes Adhes. 2010;30(5):367–79. https://doi.org/10.1016/j.ijadhadh.2010.01.005.
93. Campilho RDSG, Pinto AMG, Banea MD, da Silva LFM. Optimization study of hybrid spot-welded/bonded single-lap joints. Int J Adhes Adhes. 2012;37:86–95. https://doi.org/10.1016/j.ijadhadh.2012.01.018.
94. Wang Y, Chai P, Ma H, Zhang Y. Characteristics and strength of hybrid friction stir welding and adhesive bonding lap joints for AA2024-T3 aluminium alloy. J Adhes. 2022;98(4):325–47. https://doi.org/10.1080/00218464.2020.1832893.
95. Lu Y, Broughton J, Winfield P. A review of innovations in disbonding techniques for repair and recycling of automotive vehicles. Int J Adhes Adhes. 2014;50:119–27. https://doi.org/10.1016/j.ijadhadh.2014.01.021.
96. Markle RA, et al. Thermally reversible isocyanate-based polymers. United States Patent. US005470945A. 1995.
97. Shiote H, Sato C, Ohe M. Effects of electrical treatment conditions on dismantlable properties of joints bonded with an electrically disbonding adhesive. J Adhes Soc Japan. 2009;45(10):376–81. https://doi.org/10.11618/adhesion.45.376.
98. Leijonmarck S, Cornell A, Danielsson C-O, Åkermark T, Brandner BD, Lindbergh G. Electrolytically assisted debonding of adhesives: an experimental investigation. Int J Adhes Adhes. 2012;32:39–45. https://doi.org/10.1016/j.ijadhadh.2011.09.003.
99. Santiago D, Guzmán D, Padilla J, Verdugo P, De la Flor S, Serra À. Recyclable and reprocessable epoxy vitrimer adhesives. ACS Appl Polymer Mater. 2023;5(3):2006–15. https://doi.org/10.1021/acsapm.2c02063.
100. Banea MD, da Silva LFM, Campilho RDSG, Sato C. Smart adhesive joints: an overview of recent developments. J Adhes. 2014;90(1):16–40. https://doi.org/10.1080/00218464.2013.785916.
101. Nishiyama Y, Uto N, Sato C, Sakurai H. Dismantlement behavior and strength of dismantlable adhesive including thermally expansive particles. Int J Adhes Adhes. 2003;23(5):377–82. https://doi.org/10.1016/S0143-7496(03)00067-8.
102. Banea MD, da Silva LFM, Carbas RJC, Barbosa AQ, de Barros S, Viana G. Effect of water on the behaviour of adhesives modified with thermally expandable particles. Int J Adhes Adhes. 2018;84:250–6. https://doi.org/10.1016/j.ijadhadh.2018.04.002.
103. Bonaldo J, Banea MD, Carbas RJC, Da Silva LFM, De Barros S. Functionally graded adhesive joints by using thermally expandable particles. J Adhes. 2019;95(11):995–1014. https://doi.org/10.1080/00218464.2018.1456338.
104. Sethi S, Ge L, Ci L, Ajayan PM, Dhinojwala A. Gecko-inspired carbon nanotube-based self-cleaning adhesives. Nano Lett. 2008;8(3):822–5. https://doi.org/10.1021/nl0727765.
105. Ali MH, Batai S, Sarbassov D. 3D printing: a critical review of current development and future prospects. Rapid Prototyp J. 2019;25(6):1108–26. https://doi.org/10.1108/RPJ-11-2018-0293.
106. Rafiee M, Farahani RD, Therriault D. Multi-material 3D and 4D printing: a survey. Adv Sci. 2020;7:1902307. https://doi.org/10.1002/advs.201902307.
107. Thompson MK, Moroni G, Vaneker T, Fadel G, Campbell RI, Gibson I, et al. Design for additive manufacturing: trends, opportunities, considerations, and constraints. CIRP Ann Manuf Technol. 2016;65(2):737–60. https://doi.org/10.1016/j.cirp.2016.05.004.
108. Monzón MD, Ortega Z, Martínez A, Ortega F. Standardization in additive manufacturing: activities carried out by international organizations and projects. Int J Adv Manuf Technol. 2015;76:1111–21. https://doi.org/10.1007/s00170-014-6334-1.
109. Ulu E, Gecer Ulu N, Hsiao W, Nelaturi S. Manufacturability oriented model correction and build direction optimization for additive manufacturing. J Mech Design. 2020;142(6):062001. https://doi.org/10.1115/1.4045107.
110. Frascio M, Marques EAS, Carbas RJC, da Silva LFM, Monti M, Avalle M. Review of tailoring methods for joints with additively manufactured adherends and adhesives. Materials. 2020;13(18):3949. https://doi.org/10.3390/ma13183949.
111. da Silva LFM, Marques EAS, Campilho RDSG. Design rules and methods to improve joint strength. In: da Silva LFM, Öchsner A, Adams RD, editors. Handbook of adhesion technology. 2nd ed. Springer Cham; 2018. p. 773–810. https://doi.org/10.1007/978-3-319-55411-2_27.
112. Marques JB, Barbosa AQ, da Silva CI, Carbas RJC, da Silva LFM. An overview of manufacturing functionally graded adhesives—challenges and prospects. J Adhes. 2021;97(2):172–206. https://doi.org/10.1080/00218464.2019.1646647.
113. Packham DE. Theories of fundamental adhesion. In: da Silva LFM, Öchsner A, Adams RD, editors. Handbook of adhesion technology. Berlin: Springer; 2011. p. 9–38. https://doi.org/10.1007/978-3-642-01169-6_2.
114. Arikan E, Holtmannspötter J, Zimmer F, Hofmann T, Gudladt H-J. The role of chemical surface modification for structural adhesive bonding on polymers—Washability of chemical functionalization without reducing adhesion. Int J Adhes Adhes. 2019;95:102409. https://doi.org/10.1016/j.ijadhadh.2019.102409.
115. Shang X, Marques EAS, Machado JJM, Carbas RJC, Jiang D, da Silva LFM. Review on techniques to improve the strength of adhesive joints with composite adherends. Compos B Eng. 2019;177:107363. https://doi.org/10.1016/j.compositesb.2019.107363.
116. Sarantinos N, Tsantzalis S, Ucsnik S, Kostopoulos V. Review of through-the-thickness reinforced composites in joints. Compos Struct. 2019;229:111404. https://doi.org/10.1016/j.compstruct.2019.111404.
117. Casavola C, Cazzato A, Moramarco V, Pappalettere C. Orthotropic mechanical properties of fused deposition modelling parts described by classical laminate theory. Mater Des. 2016;90:453–8. https://doi.org/10.1016/j.matdes.2015.11.009.
118. Akhavan-Safar A, Ayatollahi MR, da Silva LFM. Strength prediction of adhesively bonded single lap joints with different bondline thicknesses: a critical longitudinal strain approach. Int J Solids Struct. 2017;109:189–98. https://doi.org/10.1016/j.ijsolstr.2017.01.022.
119. Akhavan-Safar A, da Silva LFM, Ayatollahi MR. An investigation on the strength of single lap adhesive joints with a wide range of materials and dimensions using a critical distance approach. Int J Adhes Adhes. 2017;78:248–55. https://doi.org/10.1016/j.ijadhadh.2017.08.009.
120. Castro Sousa F, Akhavan-Safar A, Goyal R, da Silva LFM. Fatigue life estimation of single lap adhesive joints using a critical distance criterion: an equivalent notch approach. Mech Mater. 2021;153:103670. https://doi.org/10.1016/j.mechmat.2020.103670.
121. Castro Sousa F, Akhavan-Safar A, Rakesh G, da Silva LFM. Fatigue life estimation of adhesive joints at different mode mixities. J Adhes. 2022;98(1):1–23. https://doi.org/10.1080/00218464.2020.1804376.
122. Dias V, Odenbreit C, Hechler O, Scholzen F, Ben ZT. Development of a constitutive hyperelastic material law for numerical simulations of adhesive steel–glass connections using structural silicone. Int J Adhes Adhes. 2014;48:194–209. https://doi.org/10.1016/j.ijadhadh.2013.09.043.

123. Van Lancker B, De Corte W, Belis J. Calibration of hyperelastic material models for structural silicone and hybrid polymer adhesives for the application of bonded glass. Construct Build Mater. 2020;254:119204. https://doi.org/10.1016/j.conbuildmat.2020.119204.
124. Ali A, Hosseini M, Sahari BB. A review of constitutive models for rubber-like materials. Am J Eng Appl Sci. 2010;3(1):232–9. https://doi.org/10.3844/ajeassp.2010.232.239.
125. Portillo FJS, Sempere ÓC, Marques EAS, Lozano MS, da Silva LFM. Mechanical characterisation and comparison of hyperelastic adhesives: modelling and experimental validation. J Appl Comput Mech. 2022;8(1):359–69. https://doi.org/10.22055/jacm.2021.38119.3242.
126. Bergström J. Mechanics of solid polymers: theory and computational modeling. William Andrew; 2015. https://doi.org/10.1016/C2013-0-15493-1.
127. Blatz PJ. Application of finite elastic theory to the behavior of rubberlike materials. Rubber Chem Technol. 1963;36(5):1459–96. https://doi.org/10.5254/1.3539651.
128. Yeoh OH. Some forms of the strain energy function for rubber. Rubber Chem Technol. 1993;66:754–71. https://doi.org/10.5254/1.3538343.
129. Ogden RW. Large deformation isotropic elasticity—on the correlation of theory and experiment for incompressible rubberlike solids. Proc Royal Soc Lond A Math Phys Sci. 1972;326(1567):565–84. https://doi.org/10.1098/rspa.1972.0026.
130. Duncan B, Dean G. Measurements and models for design with modern adhesives. Int J Adhes Adhes. 2003;23(2):141–9. https://doi.org/10.1016/S0143-7496(03)00006-X.
131. Marckmann G, Verron E. Comparison of hyperelastic models for rubber-like materials. Rubber Chem Technol. 2006;79(5):835–58. https://doi.org/10.5254/1.3547969.
132. Drass M, Schneider J. Constitutive modeling of transparent structural silicone adhesive—TSSA. Schrödter J. ed.; 2016. 14.
133. Silvestru VA, Drass M, Englhardt O, Schneider J. Performance of a structural acrylic adhesive for linear glass-metal connections under shear and tensile loading. Int J Adhes Adhes. 2018;85:322–36. https://doi.org/10.1016/j.ijadhadh.2018.07.006.
134. Sánchez-Arce IJ, Gonçalves DC, Ramalho LDC, Campilho RDSG, Belinha J. Meshless and hyper-elastic implementation to analyse flexible adhesives. Procedia Struct Integr. 2021;33:149–58. https://doi.org/10.1016/j.prostr.2021.10.019.
135. Adams RD, Coppendale J, Peppiatt NA. Failure analysis of aluminium-aluminium bonded joints. In: Allen KW, editor. Adhesion, vol. 2. Elsevier Applied Science Publishers; 1978. p. 105–20.
136. Crocombe AD, Adams RD. Influence of the spew fillet and other parameters on the stress distribution in the single lap joint. J Adhes. 1981;13(2):141–55. https://doi.org/10.1080/00218468108073182.
137. Crocombe AD. Global yielding as a failure criterion for bonded joints. Int J Adhes Adhes. 1989;9(3):145–53. https://doi.org/10.1016/0143-7496(89)90110-3.
138. Harris JA, Adams RA. Strength prediction of bonded single lap joints by non-linear finite element methods. Int J Adhes Adhes. 1984;4(2):65–78. https://doi.org/10.1016/0143-7496(84)90103-9.
139. Resende RFP, Resende BFP, Sanchez Arce IJ, Ramalho LDC, Campilho RDSG, Belinha J. Elasto-plastic adhesive joint design approach by a radial point interpolation meshless method. J Adhes. 2022;98(15):2396–422. https://doi.org/10.1080/00218464.2021.1977633.
140. Abeln B, Gessler A, Stammen E, Ilg F, Feldmann M, Dilger K, Schuler C. Strengthening of fatigue cracks in steel bridges by means of adhesively bonded steel patches. J Adhes. 2022;98(6):827–53. https://doi.org/10.1080/00218464.2021.2006059.
141. Zgoul M, Crocombe AD. Numerical modelling of lap joints bonded with a rate-dependent adhesive. Int J Adhes Adhes. 2004;24(4):355–66. https://doi.org/10.1016/j.ijadhadh.2003.11.006.
142. Akhavan-Safar A, Ayatollahi MR, Rastegar S, da Silva LFM. Impact of geometry on the critical values of the stress intensity factor of adhesively bonded joints. J Adhes Sci Technol. 2017;31(18):2071–87. https://doi.org/10.1080/01694243.2017.1297064.
143. Akhavan-Safar A, Ayatollahi MR, Rastegar S, da Silva LFM. Residual static strength and the fracture initiation path in adhesively bonded joints weakened with interfacial edge pre-crack. J Adhes Sci Technol. 2018;32(18):2019–40. https://doi.org/10.1080/01694243.2018.1458812.
144. Bogy DB. Two edge-bonded elastic wedges of different materials and wedge angles under surface tractions. J Appl Mech. 1971;38:377–87. https://doi.org/10.1115/1.3422658.
145. Qian ZQ, Akisanya AR. Wedge corner stress behaviour of bonded dissimilar materials. Theor Appl Fract Mech. 1999;32(3):209–22. https://doi.org/10.1016/S0167-8442(99)00041-5.
146. Rastegar S, Ayatollahi M, Akhavan-Safar A, da Silva L. Prediction of the critical stress intensity factor of single-lap adhesive joints using a coupled ratio method and an analytical model. Proc Inst Mech Eng L J Mater Des Appl. 2019;233(7):1393–403. https://doi.org/10.1177/1464420718755630.
147. Akhavan-Safar A, Marques EAS, Carbas RJC, da Silva LFM. Cohesive zone modelling for fatigue life analysis of adhesive joints. Springer Cham; 2022. https://doi.org/10.1007/978-3-030-93142-1.
148. Yao W, Ding R, Xu X, Liang J, Li Y, Liang C. Study on the effect of cohesive parameters on the bonding strength of the interface between the skin and 3D-mesh cloth of the automobile dash panel. J Adhes. 2022;98(16):2706–21. https://doi.org/10.1080/00218464.2021.1997746.
149. Chandra N, Li H, Shet C, Ghonem H. Some issues in the application of cohesive zone models for metal–ceramic interfaces. Int J Solids Struct. 2002;39(10):2827–55. https://doi.org/10.1016/S0020-7683(02)00149-X.
150. Alfano G. On the influence of the shape of the interface law on the application of cohesive-zone models. Compos Sci Technol. 2006;66(6):723–30. https://doi.org/10.1016/j.compscitech.2004.12.024.
151. Shen B, Paulino GH. Direct extraction of cohesive fracture properties from digital image correlation: a hybrid inverse technique. Exp Mech. 2011;51(2):143–63. https://doi.org/10.1007/s11340-010-9342-6.
152. Campilho RDSG, Banea MD, Neto JABP, da Silva LFM. Modelling adhesive joints with cohesive zone models: effect of the cohesive law shape of the adhesive layer. Int J Adhes Adhes. 2013;44:48–56. https://doi.org/10.1016/j.ijadhadh.2013.02.006.
153. May M, Voß H, Hiermaier S. Predictive modeling of damage and failure in adhesively bonded metallic joints using cohesive interface elements. Int J Adhes Adhes. 2014;49:7–17. https://doi.org/10.1016/j.ijadhadh.2013.12.001.
154. Heidari-Rarani M, Ghasemi AR. Appropriate shape of cohesive zone model for delamination propagation in ENF specimens with R-curve effects. Theor Appl Fract Mech. 2017;90:174–81. https://doi.org/10.1016/j.tafmec.2017.04.009.

155. Katsivalis I, Thomsen OT, Feih S, Achintha M. Strength evaluation and failure prediction of bolted and adhesive glass/steel joints. Glass Struct Eng. 2018;3:183–96. https://doi.org/10.1007/s40940-018-0070-0.
156. Pathak H, Singh A, Singh IV. Fatigue crack growth simulations of 3-D problems using XFEM. Int J Mech Sci. 2013;76:112–31. https://doi.org/10.1016/j.ijmecsci.2013.09.001.
157. Wells GN, Sluys LJ. A new method for modelling cohesive cracks using finite elements. Int J Numer Meth Eng. 2001;50(12):2667–82. https://doi.org/10.1002/nme.143.
158. Mergheim J, Kuhl E, Steinmann P. A finite element method for the computational modelling of cohesive cracks. Int J Numer Meth Eng. 2005;63:276–89. https://doi.org/10.1002/nme.1286.
159. Hollaway LC. Key issues in the use of fibre reinforced polymer (FRP) composites in the rehabilitation and retrofitting of concrete structures. In: Karbhari VM, Lee LS, editors. Service life estimation and extension of civil engineering structures. Woodhead Publishing; 2011. p. 3–74. https://doi.org/10.1533/9780857090928.1.3.
160. Askeland DR. The science and engineering of materials. 4th edn. Brooks/Cole; 2003.
161. Ward IM, Sweeney J. Mechanical properties of solid polymers: third edition. Wiley; 2013. https://doi.org/10.1002/9781119967125.
162. Akhavan-Safar A, Marques EAS, Carbas RJC, da Silva LFM. Fatigue Degradation Models. In: Cohesive zone modelling for fatigue life analysis of adhesive joints. Springer Cham; 2022. https://doi.org/10.1007/978-3-030-93142-1_3.
163. Carneiro Neto RM, Akhavan-Safar A, Sampaio EM, Assis JT, da Silva LFM. A customized shear traction separation law for cohesive zone modelling of creep loaded ENF adhesive joints. Theor Appl Fract Mech. 2022;119:103336. https://doi.org/10.1016/j.tafmec.2022.103336.
164. Alfrey T, Doty P. The methods of specifying the properties of viscoelastic materials. J Appl Phys. 1945;16(11):700–13. https://doi.org/10.1063/1.1707524.
165. Schwarzl F, Staverman A. Time-temperature dependence of linear viscoelastic behavior. J Appl Phys. 1952;23(8):838–43. https://doi.org/10.1063/1.1702316.
166. Xu Q, Engquist B. A mathematical model for fitting and predicting relaxation modulus and simulating viscoelastic responses. Proc Royal Soc A Math Phys Eng Sci. 2018;474(2213):20170540. https://doi.org/10.1098/rspa.2017.0540.
167. Diani J, Gilormini P, Frédy C, Rousseau I. Predicting thermal shape memory of crosslinked polymer networks from linear viscoelasticity. Int J Solids Struct. 2012;49(5):793–9. https://doi.org/10.1016/j.ijsolstr.2011.11.019.
168. Bergström JS, Rimnac CM, Kurtz SM. An augmented hybrid constitutive model for simulation of unloading and cyclic loading behavior of conventional and highly crosslinked UHMWPE. Biomaterials. 2004;25(11):2171–8. https://doi.org/10.1016/j.biomaterials.2003.08.065.
169. Pramanik R, Soni F, Shanmuganathan K, Arockiarajan A. Mechanics of soft polymeric materials using a fractal viscoelastic model. Mech Time-Depend Mater. 2022;26:257–70. https://doi.org/10.1007/s11043-021-09486-0.
170. Liu M, Fatt MSH. A constitutive equation for filled rubber under cyclic loading. Int J Non-Linear Mech. 2011;46(2):446–56. https://doi.org/10.1016/j.ijnonlinmec.2010.11.006.
171. Ayoub G, Zaïri F, Naït-Abdelaziz M, Gloaguen JM, Kridli G. A visco-hyperelastic damage model for cyclic stress-softening, hysteresis and permanent set in rubber using the network alteration theory. Int J Plast. 2014;54:19–33. https://doi.org/10.1016/j.ijplas.2013.08.001.
172. Eslami G, Movahedi-Rad AV, Keller T. Viscoelastic adhesive modeling of ductile adhesive-composite joints during cyclic loading. Int J Adhes Adhes. 2022;119:103241. https://doi.org/10.1016/j.ijadhadh.2022.103241.
173. Perzyna P. Fundamental problems in viscoplasticity. In: Chernyi GG, Dryden HL, Germain P, Howarth L, Olszak W, Prager W, et al., editors. Advances in applied mechanics. Academic Press; 1966. https://doi.org/10.1016/S0065-2156(08)70009-7.
174. G'sell C, Jonas JJ. Determination of the plastic behaviour of solid polymers at constant true strain rate. J Mater Sci. 1979;14:583–91. https://doi.org/10.1007/BF00772717.
175. Pandey PC, Narasimhan S. Three-dimensional nonlinear analysis of adhesively bonded lap joints considering viscoplasticity in adhesives. Comput Struct. 2001;79(7):769–83. https://doi.org/10.1016/S0045-7949(00)00160-7.
176. Morin D, Haugou G, Lauro F, Bennani B, Bourel B. Elasto-viscoplasticity behaviour of a structural adhesive under compression loadings at low, moderate and high strain rates. J Dynamic Behav Mater. 2015;1:124–35. https://doi.org/10.1007/s40870-015-0010-x.
177. Krairi A, Doghri I. A thermodynamically-based constitutive model for thermoplastic polymers coupling viscoelasticity, viscoplasticity and ductile damage. Int J Plast. 2014;60:163–81. https://doi.org/10.1016/j.ijplas.2014.04.010.
178. Ilioni A, Badulescu C, Carrere N, Davies P, Thévenet D. A viscoelastic-viscoplastic model to describe creep and strain rate effects on the mechanical behaviour of adhesively-bonded assemblies. Int J Adhes Adhes. 2018;82:184–95. https://doi.org/10.1016/j.ijadhadh.2017.12.003.
179. Dufour L, Bourel B, Lauro F, Haugou G, Leconte N. A viscoelastic-viscoplastic model with non associative plasticity for the modelling of bonded joints at high strain rates. Int J Adhes Adhes. 2016;70:304–14. https://doi.org/10.1016/j.ijadhadh.2016.07.015.
180. Rocha IBCM, van der Meer FP, Raijmaekers S, Lahuerta F, Nijssen RPL, Sluys LJ. Numerical/experimental study of the monotonic and cyclic viscoelastic/viscoplastic/fracture behavior of an epoxy resin. Int J Solids Struct. 2019;168:153–65. https://doi.org/10.1016/j.ijsolstr.2019.03.018.
181. Chen Y, Smith LV. A nonlinear viscoelastic–viscoplastic constitutive model for adhesives under creep. Mech Time-Depend Mater. 2022;26:663–81. https://doi.org/10.1007/s11043-021-09506-z.
182. Yu XX, Crocombe AD, Richardson G. Material modelling for rate-dependent adhesives. Int J Adhes Adhes. 2001;21(3):197–210. https://doi.org/10.1016/S0143-7496(00)00051-8.
183. Chen F, Pinisetty D, Gupta N. Study of the compressive properties of adhesively bonded carbon fiber laminates at different strain rates. J Adhes. 2022;98(16):2582–98. https://doi.org/10.1080/00218464.2021.1982706.
184. Damm J, Ummenhofer T, Albiez M. Influence of damping properties of adhesively bonded joints on the dynamic behaviour of steel structures: numerical investigations. J Adhes. 2022;98(7):934–62. https://doi.org/10.1080/00218464.2020.1865161.
185. Borges C, Nunes P, Akhavan-Safar A, Marques EAS, Carbas RJC, Alfonso L, et al. A strain rate dependent cohesive zone element for mode I modeling of the fracture behavior of adhesives. Proc Inst Mech Eng L J Mater Des Appl. 2020;234(4):610–21. https://doi.org/10.1177/1464420720904026.

186. Nunes P, Marques E, Carbas R, Akhavan-Safar A, da Silva L. DCB tests at constant strain rate using crash-resistant epoxy adhesives: a numerical and experimental approach. Proc Inst Mech Eng Part D J Automobile Eng. 2021;235(13):3234–42. https://doi.org/10.1177/0954407020954572.
187. Feng W, Xu F, Li Z, Zhang C. Mode I fracture toughness of adhesively bonded composite joints under high loading rate conditions. J Adhes. 2023;99(5):893–909. https://doi.org/10.1080/00218464.2022.2061351.
188. Akhavan-Safar A, Beygi R, Delzendehrooy F, da Silva L. Fracture energy assessment of adhesives—part I: is GIC an adhesive property? A neural network analysis. Proc Inst Mech Eng L J Mater Des Appl. 2021;235(6):1461–76. https://doi.org/10.1177/14644207211002763.
189. Delzendehrooy F, Beygi R, Akhavan-Safar A, da Silva LFM. Fracture energy assessment of adhesives Part II: is GIIc an adhesive material property? (A neural network analysis). J Adv Join Proc. 2021;3:100049. https://doi.org/10.1016/j.jajp.2021.100049.
190. Machado J, Nunes P, Marques E, Campilho R, da Silva LF. Numerical study of mode I fracture toughness of carbon-fibre-reinforced plastic under an impact load. Proc Inst Mech Eng L J Mater Des Appl. 2020;234(1):12–20. https://doi.org/10.1177/1464420719871390.
191. Challita G, Othman R. Finite-element analysis of SHPB tests on double-lap adhesive joints. Int J Adhes Adhes. 2010;30(4):236–44. https://doi.org/10.1016/j.ijadhadh.2010.02.004.
192. Zaera R, Sánchez-Sáez S, Pérez-Castellanos JL, Navarro C. Modelling of the adhesive layer in mixed ceramic/metal armours subjected to impact. Compos A Appl Sci Manuf. 2000;31(8):823–33. https://doi.org/10.1016/S1359-835X(00)00027-0.
193. Liao L, Kobayashi T, Sawa T, Goda Y. 3-D FEM stress analysis and strength evaluation of single-lap adhesive joints subjected to impact tensile loads. Int J Adhes Adhes. 2011;31(7):612–9. https://doi.org/10.1016/j.ijadhadh.2011.06.008.
194. Liao L, Sawa T, Huang C. Experimental and FEM studies on mechanical properties of single-lap adhesive joint with dissimilar adherends subjected to impact tensile loadings. Int J Adhes Adhes. 2013;44:91–8. https://doi.org/10.1016/j.ijadhadh.2013.02.007.
195. Sawa T, Nagai T, Iwamoto T, Kuramoto H. A study on evaluation of impact strength of adhesive joints subjected to impact shear loadings. In: Proceedings of the ASME 2008 International Mechanical Engineering Congress and Exposition. Volume 15: Processing and Engineering Applications of Novel Materials. 2008. p. 55–61. https://doi.org/10.1115/IMECE2008-68464.
196. Goglio L, Peroni L, Peroni M, Rossetto M. High strain-rate compression and tension behaviour of an epoxy bi-component adhesive. Int J Adhes Adhes. 2008;28(7):329–39. https://doi.org/10.1016/j.ijadhadh.2007.08.004.
197. da Costa JA, Akhavan-Safar A, Marques EAS, Carbas RJC, da Silva LFM. Cyclic ageing of adhesive materials. J Adhes. 2022;98(10):1341–57. https://doi.org/10.1080/00218464.2021.1895772.
198. Li W, Shao X, Li L, Zheng G. Effect of hygrothermal ageing on the mechanical performance of CFRP/AL single-lap joints. J Adhes. 2022;98(15):2446–73. https://doi.org/10.1080/00218464.2021.1980391.
199. Moazzami M, Ayatollahi MR, Akhavan-Safar A, da Silva LFM. Experimental and numerical analysis of cyclic aging in an epoxy-based adhesive. Polym Testing. 2020;91:106789. https://doi.org/10.1016/j.polymertesting.2020.106789.
200. Moazzami M, Ayatollahi MR, Akhavan-Safar A, Teixeira De Freitas S, Poulis JA, da Silva LF. Influence of cyclic aging on adhesive mode mixity in dissimilar composite/metal double cantilever beam joints. Proc Inst Mech Eng L J Mater Des Appl. 2022;236(8):1476–88. https://doi.org/10.1177/14644207221074696.
201. da Costa JA, Akhavan-Safar A, Marques EAS, Carbas RJC, da Silva LFM. The influence of cyclic ageing on the fatigue performance of bonded joints. Int J Fatigue. 2022;161:106939. https://doi.org/10.1016/j.ijfatigue.2022.106939.
202. Chen B, Dillard DA. The effect of the T-stress on crack path selection in adhesively bonded joints. Int J Adhes Adhes. 2001;21(5):357–68. https://doi.org/10.1016/S0143-7496(01)00011-2.
203. Ayatollahi MR, Ajdani A, Akhavan-Safar A, da Silva LFM. Effect of notch length and pre-crack size on mode II fracture energy of brittle adhesives. Eng Fract Mech. 2019;212:123–35. https://doi.org/10.1016/j.engfracmech.2019.03.024.
204. Sih GC, Macdonald B. Fracture mechanics applied to engineering problems—strain energy density fracture criterion. Eng Fract Mech. 1974;6(2):361–86. https://doi.org/10.1016/0013-7944(74)90033-2.
205. Akhavan-Safar A, Ayatollahi MR, Moazzami M, da Silva LFM. The role of T-stress and stress triaxiality combined with the geometry on tensile fracture energy of brittle adhesives. Int J Adhes Adhes. 2018;87:12–21. https://doi.org/10.1016/j.ijadhadh.2018.09.008.
206. Fleck NA, Hutchinson JW, Zhigang S. Crack path selection in a brittle adhesive layer. Int J Solids Struct. 1991;27(13):1683–703. https://doi.org/10.1016/0020-7683(91)90069-R.
207. Weissgraeber P, Leguillon D, Becker W. A review of finite fracture mechanics: crack initiation at singular and non-singular stress raisers. Arch Appl Mech. 2016;86:375–401. https://doi.org/10.1007/s00419-015-1091-7.
208. Mendoza-Navarro LE, Diaz-Diaz A, Castañeda-Balderas R, Hunkeler S, Noret R. Interfacial failure in adhesive joints: experiments and predictions. Int J Adhes Adhes. 2013;44:36–47. https://doi.org/10.1016/j.ijadhadh.2013.02.004.
209. Moradi A, Carrère N, Leguillon D, Martin E, Cognard J-Y. Strength prediction of bonded assemblies using a coupled criterion under elastic assumptions: effect of material and geometrical parameters. Int J Adhes Adhes. 2013;47:73–82. https://doi.org/10.1016/j.ijadhadh.2013.09.044.
210. Hell S, Weißgraeber P, Felger J, Becker W. A coupled stress and energy criterion for the assessment of crack initiation in single lap joints: a numerical approach. Eng Fract Mech. 2014;117:112–26. https://doi.org/10.1016/j.engfracmech.2014.01.012.
211. Weißgraeber P, Felger J, Talmon l'Armée A, Becker W. Crack initiation in single lap joints: effects of geometrical and material properties. Int J Fract. 2015;192:155–66. https://doi.org/10.1007/s10704-015-9992-6.
212. Carrere N, Martin E, Leguillon D. Comparison between models based on a coupled criterion for the prediction of the failure of adhesively bonded joints. Eng Fract Mech. 2015;138:185–201. https://doi.org/10.1016/j.engfracmech.2015.03.004.
213. Groth HL. Stress singularities and fracture at interface corners in bonded joints. Int J Adhes Adhes. 1988;8(2):107–13. https://doi.org/10.1016/0143-7496(88)90031-0.
214. Ayatollahi MR, Mirsayar MM, Dehghany M. Experimental determination of stress field parameters in bi-material notches using photoelasticity. Mater Des. 2011;32(10):4901–8. https://doi.org/10.1016/j.matdes.2011.06.002.
215. Zhang Y, Noda N-A, Takaishi K. Effects of geometry on intensity of singular stress fields at the corner of single-lap joints. World Acad Sci Eng Technol. 2011;79:911–6.
216. Borges CSP, Nunes PDP, Akhavan A, Marques EAS, Carbas RJC, Alfonso L, et al. Influence of mode mixity and loading rate on the fracture behaviour of crash resistant adhesives. Theor Appl Fract Mech. 2020;107:102508. https://doi.org/10.1016/j.tafmec.2020.102508.

217. García JA, Chiminelli A, García B, Lizaranzu M, Jiménez MA. Characterization and material model definition of toughened adhesives for finite element analysis. Int J Adhes Adhes. 2011;31(4):182–92. https://doi.org/10.1016/j.ijadhadh.2010.12.006.
218. Chousal JAG, de Moura MFSF. Mixed-mode I + II continuum damage model applied to fracture characterization of bonded joints. Int J Adhes Adhes. 2013;41:92–7. https://doi.org/10.1016/j.ijadhadh.2012.10.014.
219. Riccio A, Ricchiuto R, Di Caprio F, Sellitto A, Raimondo A. Numerical investigation of constitutive material models on bonded joints in scarf repaired composite laminates. Eng Fract Mech. 2017;173:91–106. https://doi.org/10.1016/j.engfracmech.2017.01.003.
220. Zhang Q, Cheng X, Cheng Y, Li W, Hu R. Investigation of tensile behavior and influence factors of composite-to-metal 2D-scarf bonded joint. Eng Struct. 2019;180:284–94. https://doi.org/10.1016/j.engstruct.2018.11.036.
221. Kim M-H, Hong H-S. An adaptation of mixed-mode I + II continuum damage model for prediction of fracture characteristics in adhesively bonded joint. Int J Adhes Adhes. 2018;80:87–103. https://doi.org/10.1016/j.ijadhadh.2017.10.008.
222. Sugiman S, Ahmad H. Comparison of cohesive zone and continuum damage approach in predicting the static failure of adhesively bonded single lap joints. J Adhes Sci Technol. 2017;31(5):552–70. https://doi.org/10.1080/01694243.2016.1222048.
223. Akhavan-Safar A, Marques EAS, Carbas RJC, da Silva LFM. Cohesive zone modelling—CZM. In: Cohesive zone modelling for fatigue life analysis of adhesive joints. Springer Cham; 2022. https://doi.org/10.1007/978-3-030-93142-1_2.
224. Tvergaard V, Hutchinson JW. The relation between crack growth resistance and fracture process parameters in elastic-plastic solids. J Mech Phys Solids. 1992;40(6):1377–97. https://doi.org/10.1016/0022-5096(92)90020-3.
225. da Costa JA, Akhavan-Safar A, Marques EAS, Carbas RJC, da Silva LFM. The influence of interfacial failure on the tensile S-N response of aged Arcan joints. J Appl Polymer Sci. 2022;139(16):e51991. https://doi.org/10.1002/app.51991.
226. Gastens M, Sadeghi MZ, Weiland J, Reisgen U, Schröder K-U. A methodology for detection of crack initiation in adhesively bonded joints under constant and variable amplitude fatigue loading. J Adhes. 2022;98(6):758–79. https://doi.org/10.1080/00218464.2021.1992278.
227. Houjou K, Shimamoto K, Akiyama H, Sato C. Effect of test temperature on the shear and fatigue strengths of epoxy adhesive joints. J Adhes. 2022;98(16):2599–617. https://doi.org/10.1080/00218464.2021.1982707.
228. Tan W, Jingxin N, Guangbin W, Chen H, Meng H. Effect of temperature on the fatigue performance and failure mechanism of a flexible adhesive butt joint. J Adhes. 2022;98(13):1998–2028. https://doi.org/10.1080/00218464.2021.1950537.
229. Jen Y-M. Fatigue life evaluation of adhesively bonded scarf joints. Int J Fatigue. 2012;36(1):30–9. https://doi.org/10.1016/j.ijfatigue.2011.08.018.
230. Antelo J, Akhavan-Safar A, Carbas RJC, Marques EAS, Goyal R, da Silva LFM. Fatigue life evaluation of adhesive joints in a real structural component. Int J Fatigue. 2021;153:106504. https://doi.org/10.1016/j.ijfatigue.2021.106504.
231. Beber VC, Fernandes PHE, Schneider B, Brede M, Mayer B. Fatigue lifetime prediction of adhesively bonded joints: an investigation of the influence of material model and multiaxiality. Int J Adhes Adhes. 2017;78:240–7. https://doi.org/10.1016/j.ijadhadh.2017.08.007.
232. Fernandes PHE, Poggenburg-Harrach L, Nagel C, Beber VC. Lifetime calculation of adhesively bonded joints under proportional and non-proportional multiaxial fatigue loading: a combined critical plane and critical distance approach. J Adhes. 2022;98(6):780–809. https://doi.org/10.1080/00218464.2021.2007088.
233. Shahani AR, Pourhosseini SM. The effect of adherent thickness on fatigue life of adhesively bonded joints. Fatigue Fract Eng Mater Struct. 2019;42:561–71. https://doi.org/10.1111/ffe.12931.
234. Pereira AM, Ferreira JAM, Antunes FV, Bártolo PJ. Assessment of the fatigue life of aluminium spot-welded and weld-bonded joints. J Adhes Sci Technol. 2014;28(14–15):1432–50. https://doi.org/10.1080/01694243.2012.698107.
235. Esmaeili F, Zehsaz M, Chakherlou TN, Barzegar S. Fatigue life estimation of double lap simple bolted and hybrid (bolted/bonded) joints using several multiaxial fatigue criteria. Mater Des. 2015;67:583–95. https://doi.org/10.1016/j.matdes.2014.11.003.
236. Beugre OMR, Akhavan-Safar A, da Silva LFM. Multiaxial fatigue life assessment of adhesive joints based on the concepts of critical planes: stress-based approaches. In: da Silva LFM, Adams RD, editors. 6th International Conference on Adhesive Bonding 2021. Proceedings in Engineering Mechanics. Springer Cham; 2021. https://doi.org/10.1007/978-3-030-87668-5_11.
237. Lefebvre DR, Dillard DA. A stress singularity approach for the prediction of fatigue crack initiation in adhesive bonds. Part 1: theory. J Adhes. 1999;70(1–2):119–38. https://doi.org/10.1080/00218469908010490.
238. Lefebvre D, Ahn B, Dillard D, Dillard J. The effect of surface treatments on interfacial fatigue crack initiation in aluminum/epoxy bonds. Int J Fract. 2002;114:191–202. https://doi.org/10.1023/A:1015094701018.
239. Manterola J, Leciñana I, Zurbitu J, Zabala H, Urresti I, Olave M. Lifetime prediction of bonded structural patch repairs for wind turbine pitch bearing strengthening. J Adhes. 2022;98(6):739–57. https://doi.org/10.1080/00218464.2021.2006645.
240. Monteiro J, Akhavan-Safar A, Carbas R, Marques E, Goyal R, El-zein M, et al. Influence of mode mixity and loading conditions on the fatigue crack growth behaviour of an epoxy adhesive. Fatigue Fract Eng Mater Struct. 2020;43:308–16. https://doi.org/10.1111/ffe.13125.
241. Naat N, Boutar Y, Naïmi S, Mezlini S, Da Silva LFM. Effect of surface texture on the mechanical performance of bonded joints: a review. J Adhes. 2023;99(2):166–258. https://doi.org/10.1080/00218464.2021.2008370.
242. Rocha A, Akhavan-Safar A, Carbas R, Marques E, Goyal R, El-Zein M, da Silva L. Paris law relations for an epoxy-based adhesive. Proc Inst Mech Eng L J Mater Des Appl. 2020;234(2):291–9. https://doi.org/10.1177/1464420719886469.
243. Chen Q, Guo H, Avery K, Kang H, Su X. Mixed-mode fatigue crack growth and life prediction of an automotive adhesive bonding system. Eng Fract Mech. 2018;189:439–50. https://doi.org/10.1016/j.engfracmech.2017.11.004.
244. Azari S, Papini M, Spelt JK. Effect of adhesive thickness on fatigue and fracture of toughened epoxy joints—part I: experiments. Eng Fract Mech. 2011;78(1):153–62. https://doi.org/10.1016/j.engfracmech.2010.06.025.
245. Sekiguchi Y, Sato C. Effect of bond-line thickness on fatigue crack growth of structural acrylic adhesive joints. Materials. 2021;14(7):1723. https://doi.org/10.3390/ma14071723.
246. Turon A, Costa J, Camanho PP, Dávila CG. Simulation of delamination in composites under high-cycle fatigue. Compos A Appl Sci Manuf. 2007;38(11):2270–82. https://doi.org/10.1016/j.compositesa.2006.11.009.
247. Van Paepegem W, Degrieck J. Fatigue degradation modelling of plain woven glass/epoxy composites. Compos A Appl Sci Manuf. 2001;32(10):1433–41. https://doi.org/10.1016/S1359-835X(01)00042-2.

248. Khoramishad H, Crocombe AD, Katnam KB, Ashcroft IA. Predicting fatigue damage in adhesively bonded joints using a cohesive zone model. Int J Fatigue. 2010;32(7):1146–58. https://doi.org/10.1016/j.ijfatigue.2009.12.013.
249. Moroni F, Pirondi A. A procedure for the simulation of fatigue crack growth in adhesively bonded joints based on the cohesive zone model and different mixed-mode propagation criteria. Eng Fract Mech. 2011;78(8):1808–16. https://doi.org/10.1016/j.engfracmech.2011.02.004.
250. Pirondi A, Giuliese G, Moroni F. Fatigue debonding three-dimensional simulation with cohesive zone. J Adhes. 2016;92(7–9):553–71. https://doi.org/10.1080/00218464.2015.1127764.
251. Ebadi-Rajoli J, Akhavan-Safar A, Hosseini-Toudeshky H, da Silva LFM. Progressive damage modeling of composite materials subjected to mixed mode cyclic loading using cohesive zone model. Mech Mater. 2020;143:103322. https://doi.org/10.1016/j.mechmat.2020.103322.
252. Jiang H, Gao X, Srivatsan TS. Predicting the influence of overload and loading mode on fatigue crack growth: a numerical approach using irreversible cohesive elements. Finite Elem Anal Des. 2009;45(10):675–85. https://doi.org/10.1016/j.finel.2009.05.006.
253. Serra-Aguila A, Puigoriol-Forcada JM, Reyes G, Menacho J. Viscoelastic models revisited: characteristics and interconversion formulas for generalized Kelvin-Voigt and Maxwell models. Acta Mech Sin. 2019;35:1191–209. https://doi.org/10.1007/s10409-019-00895-6.
254. Li Y, Kessler MR. Creep-resistant behavior of self-reinforcing liquid crystalline epoxy resins. Polymer. 2014;55(8):2021–7. https://doi.org/10.1016/j.polymer.2014.03.001.
255. Mainardi F, Spada G. Creep, relaxation and viscosity properties for basic fractional models in rheology. Eur Phys J Special Topics. 2011;193:133–60. https://doi.org/10.1140/epjst/e2011-01387-1.
256. Majda P, Skrodzewicz J. A modified creep model of epoxy adhesive at ambient temperature. Int J Adhes Adhes. 2009;29(4):396–404. https://doi.org/10.1016/j.ijadhadh.2008.07.010.
257. Houhou N, Benzarti K, Quiertant M, Chataigner S, Fléty A, Marty C. Analysis of the nonlinear creep behavior of concrete/FRP-bonded assemblies. J Adhes Sci Technol. 2014;28(14–15):1345–66. https://doi.org/10.1080/01694243.2012.697387.
258. Ashofteh RS, Khoramishad H. Investigation of the creep behavior of graphene oxide nanoplatelet-reinforced adhesively bonded joints. J Adhes Sci Technol. 2019;33(6):561–78. https://doi.org/10.1080/01694243.2018.1543635.
259. Dean G. Modelling non-linear creep behaviour of an epoxy adhesive. Int J Adhes Adhes. 2007;27(8):636–46. https://doi.org/10.1016/j.ijadhadh.2006.11.004.
260. Hamed E, Chang Z-T. Effect of creep on the edge debonding failure of FRP strengthened RC beams—a theoretical and experimental study. Compos Sci Technol. 2013;74:186–93. https://doi.org/10.1016/j.compscitech.2012.11.011.
261. Choi K-K, Reda Taha MM. Rheological modeling and finite element simulation of epoxy adhesive creep in FRP-strengthened RC beams. J Adhes Sci Technol. 2013;27(5–6):523–35. https://doi.org/10.1080/01694243.2012.687557.
262. Saeimi Sadigh MA, Paygozar B, da Silva LFM, Vakili Tahami F. Creep deformation simulation of adhesively bonded joints at different temperature levels using a modified power-law model. Polym Testing. 2019;79:106087. https://doi.org/10.1016/j.polymertesting.2019.106087.
263. Khabaz-Aghdam A, Behjat B, da Silva LFM, Marques EAS. A new theoretical creep model of an epoxy-graphene composite based on experimental investigation: effect of graphene content. J Compos Mater. 2020;54(18):2461–72. https://doi.org/10.1177/0021998319895806.
264. Khabazaghdam A, Behjat B, Yazdani M, Da Silva LFM, Marques EAS, Shang X. Creep behaviour of a graphene-reinforced epoxy adhesively bonded joint: experimental and numerical investigation. J Adhes. 2021;97(13):1189–210. https://doi.org/10.1080/00218464.2020.1742114.
265. Han X, Crocombe AD, Anwar SNR, Hu P. The strength prediction of adhesive single lap joints exposed to long term loading in a hostile environment. Int J Adhes Adhes. 2014;55:1–11. https://doi.org/10.1016/j.ijadhadh.2014.06.013.
266. Xu F, Arthur Jones I, Li S. A continuum damage model for transverse cracking in UD composites of linear viscoelastic behaviour. Compos Struct. 2019;225:110812. https://doi.org/10.1016/j.compstruct.2019.03.084.
267. Marques EAS, Carbas RJC, Silva F, da Silva LFM, de Paiva DPS, Magalhães FD. Use of master curves based on time-temperature superposition to predict creep failure of aluminium-glass adhesive joints. Int J Adhes Adhes. 2017;74:144–54. https://doi.org/10.1016/j.ijadhadh.2016.12.007.
268. da Silva LFM, Campilho RDSG. Advances in numerical modelling of adhesive joints. In: Advances in numerical modeling of adhesive joints. Springer; 2012. p. 1–93. https://doi.org/10.1007/978-3-642-23608-2_1.
269. Zhang L, Yalcinkaya H, Ozevin D. Numerical approach to absolute calibration of piezoelectric acoustic emission sensors using multiphysics simulations. Sens Actuator A Phys. 2017;256:12–23. https://doi.org/10.1016/j.sna.2017.01.009.
270. Katsivalis I, Feih S. Prediction of moisture diffusion and failure in glass/steel adhesive joints. Glass Struct Eng. 2022;7:381–97. https://doi.org/10.1007/s40940-022-00194-w.